



**Politecnico
di Torino**

Politecnico di Torino

Master's Degree course in Biomedical Engineering – Biomechanics

A.Y. 2022/2023

Master's Degree Thesis

**Biomechanical analysis of rowing
with different movement
constraints**

A comparison between individuals with and without physical
impairments

Supervisor:

Prof. Laura Gastaldi
Dr. Anna Cecilia Severin
Prof. Gertjan Ettema
Dr. Jørgen Danielsen

Candidate:

Denise Bentivoglio S295613

Abstract

While many studies have explored able-bodied rowing biomechanics, only a few focus on the effect of movement constraints. This study analyzes 3D kinematics and joint power during rowing under different movement constraints. Also differences between participants with and without physical impairments are explored.

Four setups are used to simulate gradually increasing movement constraints: Setup 1 - standard rowing conditions (mirrors able-bodied rowing and the PR3 para-rowing class); Setup 2 - rowing with a fixed seat, with legs still on the foot-stretcher (mirrors the PR2 para-rowing class for athletes with some residual leg functions); Setup 3 - fixed seat with legs not on the foot-stretcher (PR2 para-rowing class athletes without leg functions); Setup 4 - movement constraints applied to legs and trunk (PR1 para-rowing class).

Fourteen participants, including three with physical impairments, performed in ergometer-based sub-maximal rowing bouts in the four setups. Those without physical impairments were grouped, while those with impairments were assessed individually.

3D motion capture data was gathered at 100 Hz and forces from both the handle and the foot-stretcher of the ergometer were recorded respectively at 1500 Hz and 200 Hz. Additionally, oxygen uptake, blood lactate and perceived exertion were collected to ensure a sub-maximal intensity.

Stroke rate, stroke length, power output, and handle force were examined across the setups. Typically, the increased movement constraints led to a decrease in stroke length and handle force production. Although this necessitates a higher stroke rate for power production, power output and oxygen uptake was still decreased at roughly comparable internal exercise intensities. Participants with impairments typically showed the same behavior as the able-bodied participants. However, participant A exhibited lower stroke rate values and employed a different rowing technique with a shorter drive phase.

Abstract

Transitioning from setup 1 to setup 2 increased the range of motion in the shoulder, trunk, and pelvis. Moreover, in setup 3 and 4, trunk and shoulder range of motion was strongly reduced by constraints. Although participants with physical impairments often mirrored the able-bodied behavior, they occasionally displayed different range of motion. Particularly, participant B showed higher shoulder adduction and rotation range of motion while participant C demonstrated reduced upper limb range of motion in all planes.

Unsurprisingly, the study showed a reduction in power output in joints influenced by the constraints, such as in the trunk and leg's joints which reduce rowing performance. The relative contribution to overall power in the elbow and shoulder increased across the setups. However, with the exception of the increased shoulder power from setup 1 to setup 2, the power produced by the shoulder and elbow joints remained stable across setups, suggested no compensation occurred in response to the added constraints. This behavior in the elbow joint was also consistent among the participants with impairments, although, in the shoulder joint, from setup 3 to setup 4, they exhibited an increase in power demand.

While this research enhances our understanding of how the biomechanics of rowing change under different movement constraints, future research should encompass classified para-rowers to provide a more comprehensive overview of para-rowing biomechanics. The findings of this study strongly indicate that movement constraint has a huge impact on the ability to produce power and thereby performance in rowing, which needs to be considered during para classification.

ABSTRACT	3
LIST OF FIGURES	7
LIST OF TABLES	11
INTRODUCTION	13
1.1 ROWING HISTORY	13
1.2 ROWING AT THE OLYMPICS	14
1.3 MECHANICS OF THE ROWING STROKE	15
1.4 PARA-ROWING & CLASSIFICATION	16
LITERATURE REVIEW AND STUDY AIM	21
MATERIALS AND METHOD	25
3.1 PARTICIPANTS	25
3.2 EXPERIMENTAL SETUP	27
3.3 DATA COLLECTION	29
3.3.1 <i>Set up and equipment</i>	29
3.3.2 <i>Collection</i>	37
3.4 DATA PROCESSING	39
3.4.1 <i>QTM</i>	39
3.4.2 <i>Biomechanical model</i>	41
3.4.3 <i>Coordinate system definition</i>	43
3.4.4 <i>Joint definition</i>	48
3.4.5 <i>Time-normalization and statistics</i>	50
3.4.6 <i>Stroke rate, Stroke length and Drive phase duration</i>	50
3.4.7 <i>Kinematic data processing</i>	51
3.4.8 <i>Kinetic data processing</i>	53
RESULTS AND DISCUSSION	57
4.1 STROKE LENGTH, STROKE RATE, AND TOTAL POWER	60
4.2 FORCE HANDLE	62
4.3 TOTAL POWER GENERATED BY THE ROWER	65
4.4 RANGE OF MOTION	67

<i>4.4.1 Elbow</i>	<i>68</i>
<i>4.4.2 Shoulder and Trunk</i>	<i>71</i>
<i>4.4.3 Pelvis</i>	<i>76</i>
<i>4.4.4 Thigh</i>	<i>78</i>
<i>4.4.5 Knee and Ankle</i>	<i>80</i>
4.5 JOINT'S POWER	84
CONCLUSIONS	95
REFERENCES	97

List of figures

Figure 1 -Rowing positions and phases [2]	15
Figure 2 – Para-rowing classification in the PR1, PR2 and PR3 classes [1].	19
Figure 3 - Setup 1 seat configuration; conventional ergometer.	27
Figure 4- Setup 2 seat configuration; fixed seat.	28
Figure 5 - Setup 3 seat configuration; fixed seat, feet placed outside the foot- stretcher and backrest with a low belt.....	28
Figure 6 - Setup 4 seat configuration; fixed seat, feet placed outside the foot- stretcher, backrest with upper and lower belt.....	29
Figure 7 - Human body with markers' position. Each marker is identified by its respective label name. Notably, markers highlighted in red are exclusively present in setup 1 and setup 2.	33
Figure 8 - Ergometer with markers' placement. Each marker is identified by its respective label name.	34
Figure 9 - Free body diagram of the rower with the external forces.....	37
Figure 10 - Segment definition distinct based on the setup. Illustration with segment ID and marker ID, tables with segment and markers explanation.....	41
Figure 11 - Inertial Coordinate System (ICS).	43
Figure 12 - Forearm segment LCS. Anterior view of the forearm and arm. Axis of the forearm LCS (Local Coordinate System) and the placement of markers.	44
Figure 13 - Trunk segment LCS. Posterior and the left side view of the trunk and pelvis. Axis of the trunk LCS (Local Coordinate System) and the placement of markers.	45
Figure 14– Arm segment LCS. Anterior view of the forearm and arm. Axis of the arm LCS (Local Coordinate System) and the placement of markers	45
Figure 15 - Up-trunk segment LCS. Posterior and the left side view of the trunk and pelvis. Axis of the up-trunk LCS (Local Coordinate System) and the placement of markers.	46

List of figures

Figure 16 -Thigh segment LCS. Anterior and the left side view of the thigh. Axis of the thigh LCS (Local Coordinate System) and the placement of markers.....	46
Figure 17 - Shank segment LCS. Medial and the anterior view of the shank and foot. Axis of the shank LCS (Local Coordinate System) and the placement of markers.	47
Figure 18 - Foot segment LCS. Medial and anterior view of the shank and foot. Axis of the foot LCS (Local Coordinate System) and the placement of markers.....	47
Figure 19 - Stroke Length LS, Stroke Rate SR, Power generated by the rower. AB participants are reported in grey, while mean \pm SD of the AB group is reported in black. Participants with physical impairments are reported separately as PartA, PartB, and PartC with the colors in the legend.	60
Figure 20 - Force handle among the four setups. AB participants are reported in gray, AB mean \pm SD is reported in black and participants with physical disabilities are reported with different colors as in the legend.	62
Figure 21 – The grid graph displays the handle force for all participants within the AB group. This visualization is valuable for discerning variations in rowing techniques among the participants.	63
Figure 22 - Power generated by the rower, calculated as outlined in Section 3.4.9.....	65
Figure 23 -ELBOW ROM [deg]: Flexion/Extension, Pronation/Supination. AB participants are reported in grey, while mean \pm SD of the AB group is reported in black. Values for participants with physical impairments are presented as mean \pm SD, with colors corresponding to the legend.	68
Figure 24 - SHOULDER ROM [deg]: Flexion/Extension, Adduction/Abduction, Medial/Lateral rotation. AB participants are reported in grey, while mean \pm SD of the AB group is reported in black. Values for participants with physical impairments are presented as mean \pm SD, with colors corresponding to the legend.	71
Figure 25 - TRUNK ROM [deg]: Flexion/Extension, lateral trunk flexion Right/Left, Right/Left Rotation. AB participants are reported in grey,	

List of figures

- while mean \pm SD of the AB group is reported in black. Values for participants with physical impairments are presented as mean \pm SD, with colors corresponding to the legend..... 72
- Figure 26- PELVIS ROM [deg]: Flexion/Extension, Lateral pelvis flexion Right/Left, Right/Left Rotation. AB participants are reported in grey, while mean \pm SD of the AB group is reported in black. Values for participants with physical impairments are presented as mean \pm SD, with colors corresponding to the legend. The pelvis angle is analyzed only in setup 1 and 2, and consequently, PartB and PartC are not included in the analysis..... 76
- Figure 27 - THIGH ROM [deg]: Flexion/Extension, Adduction/Abduction, Medial/Lateral rotation. AB participants are reported in grey, while mean \pm SD of the AB group is reported in black. Values for participants with physical impairments are presented as mean \pm SD, with colors corresponding to the legend. The thigh angle is analyzed only in setup 1 and 2, and consequently, PartB and PartC are not included in the analysis..... 78
- Figure 28 - KNEE ROM [deg]: Flexion/Extension, Medial/Lateral rotation. AB participants are reported in grey, while mean \pm SD of the AB group is reported in black. Values for participants with physical impairments are presented as mean \pm SD, with colors corresponding to the legend. The knee angle is analyzed only in setup 1 and 2, and consequently, PartB and PartC are not included in the analysis..... 80
- Figure 29 - ANKLE ROM [deg]: dorsiflexion/plantarflexion, inversion/eversion, medial/lateral rotation. AB participants are reported in grey, while mean \pm SD of the AB group is reported in black. Values for participants with physical impairments are presented as mean \pm SD, with colors corresponding to the legend. The ankle angle is analyzed only in setup 1 and 2, and consequently, PartB and PartC are not included in the analysis..... 81
- Figure 30 – Relative power in the upper body joints [%]: elbow, shoulder and L5-S1/T8 joint. AB participants are reported in grey, while mean \pm SD of the AB group is reported in black. Values for participants with

List of figures

physical impairments are presented as mean \pm SD, with colors corresponding to the legend..... 85

Figure 31 - Relative power in the lower body joints [Watt]: hip, knee and ankle. AB participants are reported in grey, while mean \pm SD of the AB group is reported in black. Values for participants with physical impairments are presented as mean \pm SD, with colors corresponding to the legend. The lower body is analyzed only in setup 1 and 2, and consequently, PartB and PartC are not included in the analysis..... 86

Figure 32 - Power in the upper body joints [Watt]: elbow, shoulder and L5-S1/T8 joint. AB participants are reported in grey, while mean \pm SD of the AB group is reported in black. Values for participants with physical impairments are presented as mean \pm SD, with colors corresponding to the legend. 87

Figure 33 - Power in the lower body joints [Watt]: hip, knee and ankle. AB participants are reported in grey, while mean \pm SD of the AB group is reported in black. Values for participants with physical impairments are presented as mean \pm SD, with colors corresponding to the legend. The lower body is analyzed only in setup 1 and 2, and consequently, PartB and PartC are not included in the analysis..... 88

List of tables

Table 1- Participants with physical impairments.....	26
Table 2 – Able-bodied participants	26
Table 3 - The table provides details on the body markers and on the markers applied on the ergometer, including their label names and corresponding position descriptions. Additionally, it contains information regarding the presence or absence of markers for various setups. In the table, a checkmark (✓) signifies that the marker is present during that setup, an "X" indicates the marker's absence, and "R" denotes that the marker position is reconstructed later using other markers as references.....	36
Table 4 – A comprehensive overview of joint definitions, emphasizing the segments associated with each joint and the Degrees of Freedom (DOF) for each joint.	49
Table 5 - Rotation axis names for each joint. These are presented in the Local Coordinate System (LCS) of the proximal segment for reference.	49
Table 6 - Nomenclature convention employed to denote the angles of the body segments based on the Local Coordinate System (LCS) used for their expression.	51
Table 7 – This table illustrates the two analyzed chains used for power calculations in the joints. It provides details on the point of application of distal forces used for force and power calculations in each joint, while also highlighting variations across different setups.	54
Table 8 – Anthropometric measures from P. De Leva (1996). Mass is the mass (%) of the segment relative to the body mass; Longitudinal COM position and radii of gyration are both relative to the respective segment length.	55
Table 9- Performance and physiological variables presented as single values or mean \pm SD for the participants in the four different setups.	58
Table 10 - Range of Motion (ROM)of the elbow, expressed in degree. Values are reported as mean \pm SD. The elbow angle is considered between the forearm segment and the arm segment.	69

List of tables

Table 11 - Range of Motion (ROM)of the shoulder, expressed in degree. Values are reported as mean \pm SD. The shoulder angle is considered between the arm segment and the trunk/up-trunk segment.	73
Table 12 - Range of Motion (ROM)of the trunk, expressed in degree. Values are reported as mean \pm SD. The trunk angle is considered between the trunk/up-trunk segment and the ICS.....	73
Table 13 - Range of Motion (ROM)of the pelvis, expressed in degree. Values are reported as mean \pm SD. The pelvis angle is considered between the pelvis segment and the ICS.	77
Table 14 - Range of Motion (ROM)of the thigh, expressed in degree. Values are reported as mean \pm SD. The thigh angle is considered between the thigh segment and the ICS.....	79
Table 15 - Range of Motion (ROM)of the knee, expressed in degree. Values are reported as mean \pm SD. The knee angle is considered between the shank segment and the thigh segment.....	82
Table 16 - Range of Motion (ROM)of the ankle, expressed in degree. Values are reported as mean \pm SD. The ankle angle is considered between the foot segment and the shank segment.....	82
Table 17 – This table serves as a reminder of the conventions utilized to define power in the various joint. It provides a clear delineation of joints belonging to the upper and lower body. Additionally, it underscores the adopted convention for expressing power in both the L5-S1 joint and the T8 joint.	84
Table 18 – Relative power of the body joints, expressed in %. Values are reported as mean \pm SD. Some L5-S1/T8 joint values in setup 4 are excluded from reporting due to being zero.	89
Table 19 - Power of the body joints, expressed in Watt. Values are reported as mean \pm SD. Some L5-S1/T8 joint values in setup 4 are excluded from reporting due to being zero.	89

Chapter 1

Introduction

1.1 Rowing history

Rowing, often touted as one of the oldest sporting traditions in the world, has a history that transcends centuries and continents. Its roots, which initially lay in practical applications such as transportation and warfare, have since grown into a global sporting phenomenon, ingrained in the cultural fabric of English-speaking societies.

Long before the wheel revolutionized human transportation, the oar stood as one of the most groundbreaking inventions. Evidence of early rowing boats dates back to a staggering 5800 BC, with the first known representation discovered in Finland [3]. These early vessels were instrumental in facilitating trade, exploration, and warfare across waterways. However, it was in the serene canals of Venice, Italy, where the seeds of competitive rowing were sown. In 1315, the world witnessed its inaugural regatta, a thrilling showdown between gondoliers and boatmen competing in various types of rowing boats. This event marked the birth of regattas as we know them today, igniting a spirit of competition on the water that would spread far and wide.

Rowing continued to evolve wherever people and water converged, but its modern form as a sport took shape in England during the 1700s. The English affinity for the sport would ultimately lead to the development of one of rowing's most iconic events, the Oxford versus Cambridge University Boat Race. This celebrated race, first held in 1829 on the River Thames, would become synonymous with the sport and set the standard for competitive rowing.

Chapter 1 - Introduction

In the modern era, rowing has ascended to the pinnacle of athletic achievement, securing its place as an amateur sport and an Olympic event. The transformation of rowing into a global competitive discipline was prompted by Pierre de Coubertin in 1896, the visionary founder of the Modern Olympics.

Remarkably, rowing is one of the five sports to have been a consistent presence in every modern Olympic Games. The inclusion of inrigger fours in the 1912 Olympics marked another milestone and, women's rowing made its debut in 1976. Despite these additions, rowing maintains its status as the third-largest sport in terms of participant quota, following athletics and swimming [4].

In 2005, the Paralympics embraced adaptive rowing, reflecting the sport's increasing popularity and inclusivity on a global scale.

1.2 Rowing at the Olympics

In the modern era of the Olympics, rowers compete in a 2000-meter race, either as individuals, pairs, fours or eights.

One of the defining features of Olympic rowing is the variety of boat configurations that athletes utilize. These configurations are tailored to accommodate different number of rowers, each with its own set of challenges and strategies.

Rowing typically encompasses two distinct categories: *sculling* and *sweep* rowing. The primary distinction between these categories lies in the technique employed. Sculling necessitates the use of two oars, one grasped in each hand, while in contrast, sweep rowing involves rowers handling a single oar held with both hands.

The Paris 2024 Olympic regatta will include an even split of seven women's and men's events.

- Single Sculls: rowers go solo, scull rowing
- Pair: two rowers, sweep rowing
- Double Sculls: two rowers, scull rowing

Chapter 1 - Introduction

- Coxless Four: four rowers, sweep rowing
- Quadruple Sculls: four rowers, scull rowing
- Eight: eight rowers, sweep rowing. In addition to the physical prowess of rowers, these boats include a coxswain, a critical member who not only steers the boat but also guides and motivates the crew. The coxswain's control over the boat's direction is facilitated by a small rudder attached to the foot of one of the rowers, connected by a cable. This arrangement ensure that the crew navigates the course with utmost precision.
- Lightweight double sculls: two rowers, scull rowing, lightweight boat

1.3 Mechanics of the rowing stroke

Biomechanics is the application of the principles and concepts of classical mechanics to biological systems. In the context of rowing, it involves comprehending the interaction between the body, oars, and the environment to efficiently generate force and propulsion through coordinated muscle actions [5, 6]. This understanding is crucial for deciphering the mechanisms behind rowing power output [7] and may contribute to distinguishing athletes based on their performance levels or specific para-athlete classifications. This allows coaches to identify and correct technique, which is essential for optimizing performance and reducing the risk of injury [8, 9].

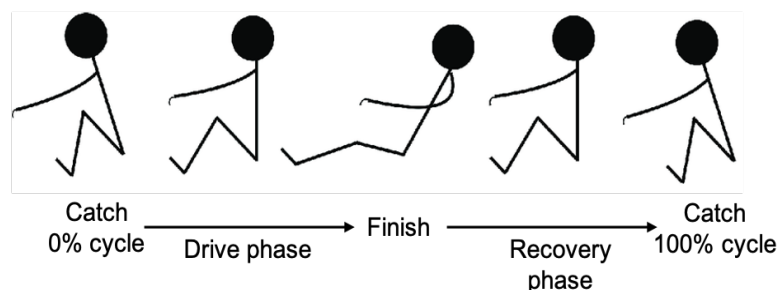


Figure 1 -Rowing positions and phases [2]

Chapter 1 - Introduction

Rowing is a cyclic movement with repetitive strokes. Typically, each stroke is divided into two phases – drive and recovery – where the drive starts at catch and ends at the finish event, while recovery lasts from finish until the next catch event [10-12]. The driving phase starts with the catch event, where the rowers are in the forward most position of the boat with their knees in the flexed and compacted position while the elbows are extended [13] and the oar is fully immersed into the water. The catch event coincides with the moment the rower starts pushing on the foot stops and pulling the oar handle [11]. During the driving phase, the trunk of the rower rotates anteriorly at the pelvis and legs extend actively while the rower pulls the oar handle towards his chest or abdomen [11]. The driving phase finishes with the finish event where rowers are in the back most position of the boat with their knees completely extended, elbows flexed and the oar blade out of the water [12]. The finish event coincides with the beginning of the recovery phase [5]. In this phase rowers pushing the end of the oar away from their bodies, flex their knees while moving forward on the sliding seat maintaining the blade of the oar out of the water [10, 12].

During the stroke, the primary hindrance to the boat's forward movement is mainly attributed to water and air resistance, commonly referred to as drag [14]. Understanding drag is essential for rowers and coaches. Skin drag (friction between the boat's surface and water) and form drag (turbulence due to the hull's shape) increase with boat velocity, and this increase is proportional to the square of velocity, making higher speeds significantly more challenging to achieve. Furthermore, the only time when rowers can increase the system speed is during the drive phase, and only when more than half of the blade is submerged in the water [14].

1.4 Para-rowing & classification

Para-rowing represents the Paralympic adaptation of the sport of rowing, catering to athletes with functional or visual impairments [15]. Para-rowing made its debut in the Paralympic Games in Beijing in 2008, with athletes

Chapter 1 - Introduction

competing in a 1000-meter distance race [16]. However, in 2017, the race distance was altered to 2000-meters to better align it with rowing at the Olympic Games [17].

Athletes eligible for participation in para-rowing are categorized into distinct classes based on the nature of their impairments. This ensure that athletes compete against others with similar capabilities, promoting fair and equitable competition while accounting for the wide range of disabilities within the sport.

As reported in the World Rowing Classification Manual, the para-rowing classification system involves a comprehensive evaluation of an athlete's functional capabilities and impairments, leading to the assignment of specific classification category. During the process of classification, athletes begin with an initial assessment to determine their eligibility. This assessment encompasses a thorough medical examination and a functional evaluation to assess the athlete's abilities and limitations. Expert classification panels, comprising medical professionals and technical expert work collaboratively to evaluate and classify athletes. These panels are instrumental in ensuring the accuracy and fairness of the classification process.

The functional classification system, updated in line with the latest guidelines, recognizes three primary categories in para-rowing:

- PR3-PI Class: These athletes possess functional use of their legs, trunk, and arms for rowing and can effectively employ the sliding seat to propel the boat forward. They have impairments affecting their joint mobility, strength, or coordination that affect their ability to generate sufficient force during the rowing stroke [18].
- PR2 Class: Athletes in this category possess functional trunk movement, but necessitate the use of a fixed seat to participate effectively. The PR2 class caters to athletes with joint, strength, or coordination impairments that prevent them from using their leg during the recovery phase [18].

Chapter 1 - Introduction

- PR1 Class: Athletes in the PR1 class primarily rely on their arms and shoulder to apply force for rowing. The PR1 classification is aimed to athletes who have joint, strength, or coordination impairments that significantly affect their ability to utilize their trunk and leg drive required in the rowing stroke [18].

To assess an athlete's classification, the panels employ a comprehensive approach, incorporating medical assessments, functional tests, and on-water evaluations to ascertain how an athlete's impairment impacts their rowing performance. The ultimate objective of the classification system is to ensure that athletes compete against others with similar level of impairment.

The accessibility of para-rowing is made possible by the use of adaptive equipment. Specialized boats, often equipped with increased stability, modified oars and customized seating, are designed to accommodate various levels of physical impairment. In addition, assistive devices such as straps and braces are often used to optimize the athlete's ability to row effectively [11, 19]. Particularly, all straps used in para-rowing should be single-point release with no mechanical buckles, so they can be unmade in a quick-release fashion in case of boat capsizing [20]. These boat and seat adaptations allow athletes to fully engage in the sport and maximize their performance [11].

In the Para-Olympic Games, para-rowing's classes differ slightly from those in the Olympic competition [17]. In the scull rowing category, para-rowing includes the following boat classes: PR1 Single scull, PR2 Single scull, PR2 Mixed double scull, and PR3 Mixed double scull. While in the sweep rowing category, para-rowing includes PR3 Coxless Pair and PR3 Mixed Coxed Four.

Chapter 1 - Introduction

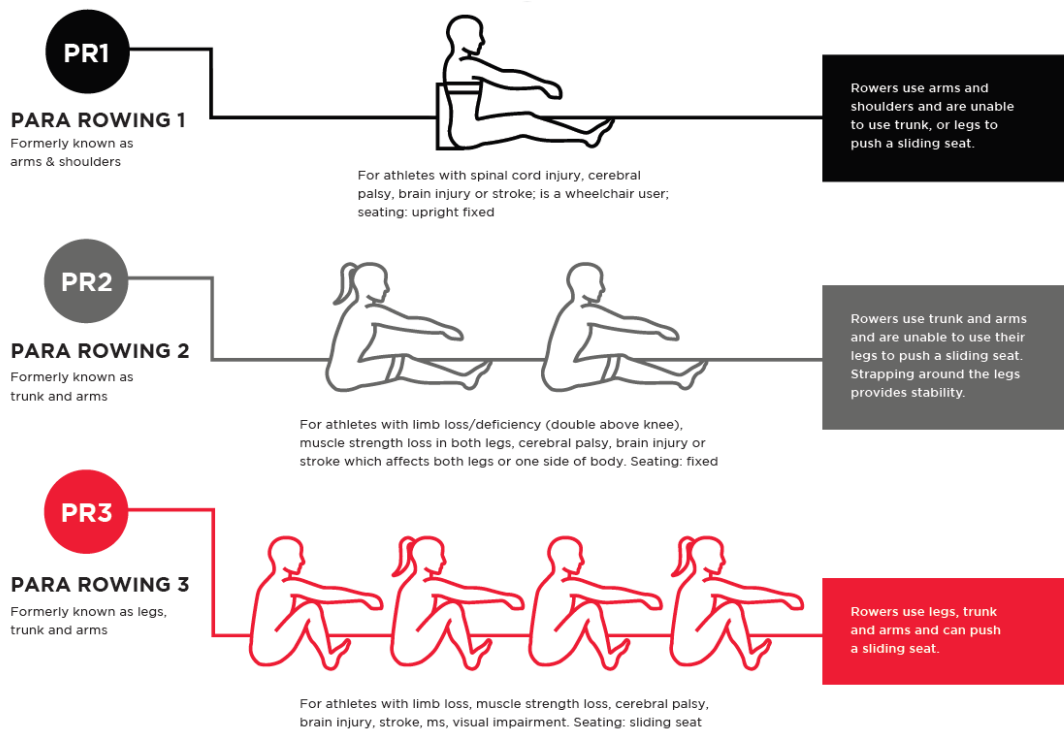


Figure 2 – Para-rowing classification in the PR1, PR2 and PR3 classes [1].

Chapter 2

Literature review and study aim

Rowing is defined as a cyclic sport consisting of a rowing stroke, which includes two phases: the drive and the recovery [21, 22], alternate by two distinct events known as the catch and the finish [21, 22]. The rowing strokes initiates with the catch event, followed by the drive phase, the finish event, and subsequently the recovery phase, all of which are then repeated in the same sequence [14, 23]. During the drive phase, the propulsive force necessary to propel the boat forward is generated [7, 12, 14].

For rowers with physical or visual impairment [17], para-rowing, also known as adaptive rowing, was first raced at the 2002 World Rowing Championships in Seville [17]. It was subsequently introduced into the Paralympic program in 2005 and it made its debut at the 2008 Paralympic regattas in Beijing, where athletes competed in 1000-meter races. In 2017, a rule change doubled the racing distance, bringing para-rowing in line with the distances of Olympic rowing competitions [17, 24]

In an attempt to ensure that athletes compete against others with similar capabilities, rowers eligible for participation in para-rowing are categorized into three distinct classes based on the nature of their impairments. These classes are defined by the World Rowing Instructional Manual for Para-Rowing [18] and divide rowers according to the different impairments: individuals with legs, trunk and arms (LTA) abilities fall into the PR3 class, individuals with trunk and arms (TA) abilities are categorized as PR2, and individuals with arms and shoulder (AS) abilities are classified under PR1.

Diverse levels of impairment necessitate tailored support mechanisms to ensure safety and stability during the rowing activity [25, 26]. Specifically, in the PR3 class, rowers have functional use of their legs, enabling them to

Chapter 2 - Literature review and study aim

effectively utilize the sliding seat to propel the boat forward [18]. In contrast, rowers in the PR2 and PR1 classes do not have the ability to use the sliding seat; therefore, the seat is fixed to facilitate their effective participation and legs are strapped at the thigh level [18]. Furthermore, rowers with abilities only in the arms and shoulder, classified as PR1, necessitate the utilization of trunk support mechanism [18].

In the context of laboratory research dedicated to the examination of para-rowing, ergometers are a standard fixture as in the examination of rowing [2, 12, 21, 27, 28]. They undergo adaptations [11, 29] that may encompass various aspects, such as measures to secure the seat to prevent unintended movements to simulate the class PR2 and the introduction of constraints like a backrest to simulate the class PR1.

In the literature, there is a limited number of studies that have been explored the impact of these specific restrictions on the biomechanics. And on the para-rowing performance. Notably, the study conducted by Cutler et al. in 2017 [11] represent the first research effort to document kinematic and kinetic alterations associated with para-rowing setups, utilizing able-bodied athletes as subjects. It has been observed that using PR2 or PR1 boat configurations, can impact the range of motion even when employed by able-bodied athletes [11]. Yet, there remains a gap in understanding how these movement constraints affect joint range of motion differently in able-bodied individuals compared to individuals with physical impairments. Indeed, the challenge of grouping a sufficiently large group of para-athletes for comprehensive research is a significant one. In response to this challenge, a viable solution, as seen in other research fields, is to continue utilizing able-bodied participants as part of the analysis while also incorporating individuals with physical impairments into the study, following a model similar to that employed in studies such as the one conducted by Bezodis et al. in 2020 [30]. This approach facilitates a more inclusive and comprehensive examination of the various factors that influence para-rowing performance.

When assessing rowing performance, various variables can be considered for analysis as reported in the literature [31, 32]. One variable of interest is the total power generated by the rower, strictly connected with the force

Chapter 2 - Literature review and study aim

generated from the rower on the handle and on the foot-stretcher, a concept demonstrated in the study conducted by Hofmijster et al. in 2007 [33]. Thus, higher power is typically indicative of better performance [5, 31, 33]. However, it is noteworthy that current literature does not encompass investigations into how rowing power production is altered when applying movement restrictions to simulate para-rowing conditions. This represents an area where further research is warranted to comprehensively understand the impact of such restrictions on rowing performance.

The aim of this study is to delve into the examination of the influence of movement restrictions on ergometer rowing biomechanics and to compare individuals with and without physical impairments. A significant aspect of this investigation centers on the assessment of 3D body segments kinematics, as well as the analysis of the power generated by body joints. We aim to determine whether the imposition of movement constraints leads to an increased demand for power production from specific joints that are free to move, such as the shoulder and elbow. Furthermore, we anticipate that the application of movement constraints will diminish the capacity to generate rowing power, particularly from the lower body, concomitantly reducing the force exerted while pulling the handle.

Chapter 3

Materials and Method

3.1 Participants

Fifteen participants were recruited, for whom the inclusion criteria were:

- 1) Physically active individuals with experience in training on a rowing ergometer,
- 2) age from 18 to 40 years,
- 3) with and without physical impairment,
- 4) no conditions of cognitive impairment affecting the ability to follow the test protocol and instructions.

Data of fourteen participants are analyzed, one of them was removed due to issue with the data quality. Particularly, three individuals with impairments, defined in this study with the letters A,B and, C as reported in (Table 1) and eleven individuals without disabilities, defined in this study as Able-Bodied (AB), (Table 2)(8 males, 3 females mean \pm SD: age 27.9 ± 6.3 years; height 182.1 ± 7.3 cm; body mass 77.7 ± 13.7 kg) was accepted for analysis.

All participants were well-trained, not specifically in rowing but with experience on an ergometer, and in good health and free of injuries during the testing period. The exact training status and overall amount of physical activity each participant performed regularly was not known. Data collection was conducted at the movement laboratory at SenTIF (Centre for Elite Sports Research) in Trondheim. Ethical approval was obtained from Norwegian Centre for Research Data (NSD, ID number: 366991), and the data collection was conducted in accordance with the ethical standards by the Norwegian National Committee for Medical and Health research ethics and the Declaration of Helsinki.

Chapter 3 - Materials and Method

Table 1- Participants with physical impairments

Participant ID	Gender	Age	Body mass [kg]	Height [cm]	Clinical diagnosis
A	M	34	95.0	183	CNS Vasculitis at the L1-L2 level
B	F	24	62.0	156	Ehlers-Danlos syndrome
C	F	25	60.7	164	Spinocerebellar ataxia
n=3					

Table 2 – Able-bodied participants

Participant ID	Gender	Age	Body mass [kg]	Height [cm]
AB1	M	22	72.0	180
AB2	F	23	53.0	167
AB3	M	29	69.1	182
AB4	M	29	85.5	196
AB5	M	36	82.9	183
AB6	F	25	62.5	181
AB7	F	25	69.7	179
AB8	M	30	80.0	176
AB9	M	22	98.5	187
AB10	M	24	90.0	186
AB11	M	42	91.5	186
n=11				
Mean	8M/3F	27.9	77.7	182.1
σ		6.3	13.7	7.3
Max		42	98.5	196
Min		22	53.0	167

3.2 Experimental setup

In the course of this research, the investigation centers on the biomechanical response of four distinct rowing conditions, which we have designated as “setups”. These setups are designed to explore and simulate the different categories of para-rowing and comprised the following configurations:

- 1) Setup 1 - Standard ergometer setup: this condition retains the conventional ergometer where the flywheel and the stretcher are fixed and only the seat moves. The participant sits on the sliding seat without strapping and feet are secured into the foot-stretcher. This setup provides a baseline for comparison against the other three configurations. It allows for the simulation of normal/AB rowing and corresponds to the PR3 class in para-rowing, where athletes have full functionality of their legs (Figure 3).

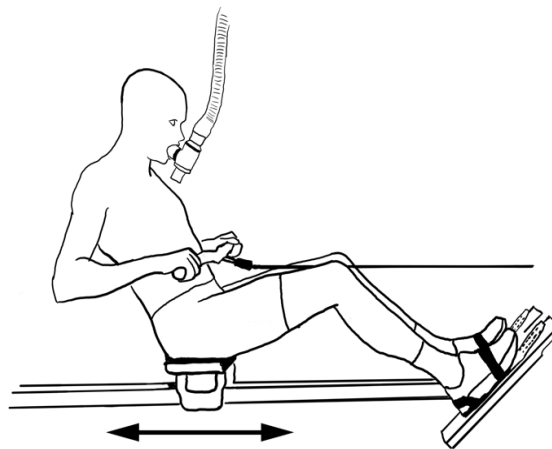


Figure 3 - Setup 1 seat configuration; conventional ergometer.

- 2) Setup 2 - Legs, Trunk, Arm - Fixed seat and foot-stretcher: The second setup replicates the first one, with the distinction that it introduces a constraint on the seat, preventing it from sliding (as depicted in Figure 4). This adjustment is designed to investigate the effects of partially immobilized lower limbs while maintaining full trunk functionality. It simulates the PR2 class in para-rowing, where athletes still retain some level of leg function.

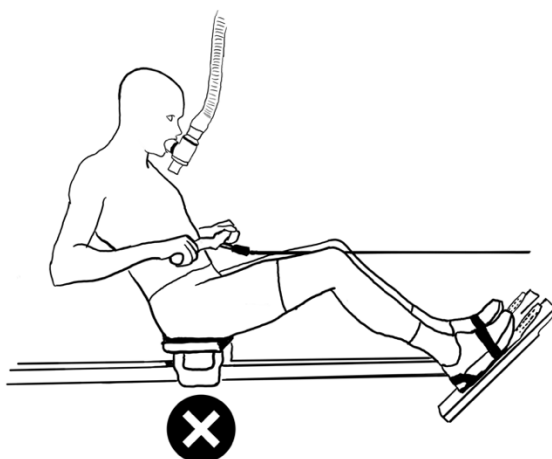


Figure 4- Setup 2 seat configuration; fixed seat.

- 3) Setup 3 - Trunk, Arm - Fixed seat, backrest and foot placement: The third setup features a fixed seat, a foot placement outside of the foot-stretcher, and a backrest with a low belt providing lower trunk support (Figure 5). Additionally, participants' calves are supported on an auxiliary platform, restricting completely the use of the lower body. For this reason, to secure the participant, a lower trunk support is needed. This configuration's objective is to explore the PR2 class in para-rowing, where participants do not have leg function.

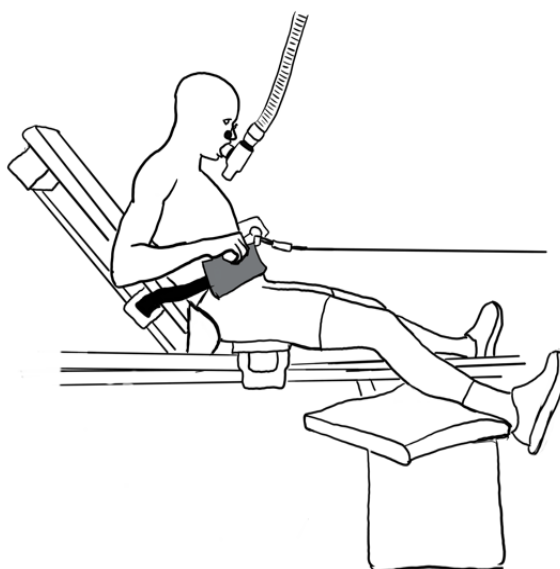


Figure 5 - Setup 3 seat configuration; fixed seat, feet placed outside the foot-stretcher and backrest with a low belt.

- 4) Setup 4 - Arm - Enhanced support with upper belt using only arms:
The fourth setup features a fixed seat, a backrest with lower and upper belt secure, and foot placement outside of the foot-stretcher (Figure 6). The backrest gives a complete support to the trunk. This setup is comparable to the PR1 class in para-rowing. Participants are thereby required to row solely using their upper extremities comparable to the PR1 class in para-rowing.

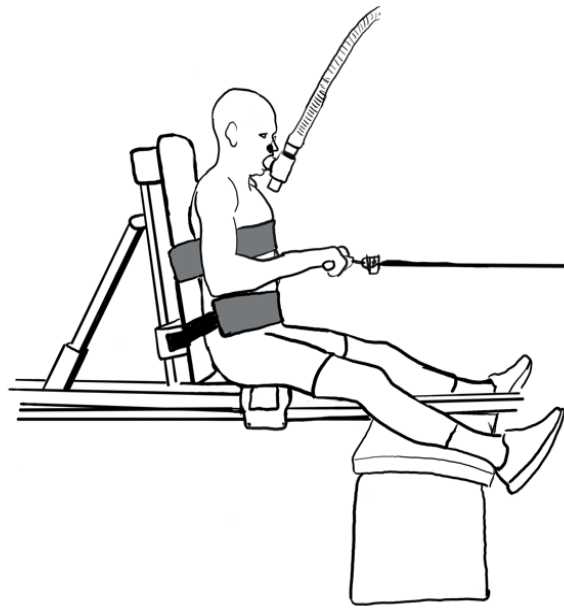


Figure 6 - Setup 4 seat configuration; fixed seat, feet placed outside the foot-stretcher, backrest with upper and lower belt.

These configurations allow us to simulate the para-rowing classes while studying the physiological and performance responses of participants.

3.3 Data collection

3.3.1 Set up and equipment

The rowing trials were performed using a Row Perfect 3 (RP3) ergometer (Care RowPerfect3 Bv., The Netherlands). Rowing was performed using the flywheel as resistance and the stretcher fixed with only the seat moving. The experiment took place in two different days, where during Day 1 participants underwent a familiarization process with the ergometer in the four setups.

Chapter 3 - Materials and Method

The main experiments took place on Day 2 and consisted of 4-minutes rowing bouts at submaximal at each setup. Thus, all participants performed their rowing bouts at approximately similar internal exercise intensities (relative heart rate) but at different power outputs. During the rowing bouts, each athlete was instructed to row at approximately a constant power output which was based on Day 1 familiarization protocol.

The damper of the flywheel was set at the lowest setting for all the participants. This chosen setting remained consistent throughout the entire procedure, maintaining uniformity across the protocol (i.e at all setups). A mobile phone (Apple Inc., Cupertino, California, United States) connected to the ergometer, displayed duration, split (how long it will take to row 500 meters at the current speed), distance and power output per stroke through the RP3 Rowing app (RP3 Rowing). This enabled rowers to row at the prescribed stroke rate and power for each specific condition.

Different setups of the ergometer were used during the protocol, due to that, for all the setups except setup 1, the seat was fixed using straps and an appropriate distance from the foot-stretcher decided by the participant based on personal preference. For setup 3 and setup 4 was added a backrest handcrafted equipped with two belts placed at waist and chest level and a support for the legs. The inclination angle of the backrest was changed between the two setups, in particular during setup 3 the inclination of the backrest was such that it did not interfere with the movement of the participant and only served as support at pelvic level. Instead, in setup 4, the backrest was positioned vertically to block totally the trunk and preventing its movement. The leg support comprised a stepper with two pillows placed on top. Participants rested their calves on these pillows with their legs fully extended. However, participants A, B and C performed in setup 3 and setup 4 with their feet securely strapped to the foot-stretcher to prevent any risk of falling. Consequently, in setup 3, they rowed with the leg positioning similar to setup 2 but with the added security of the waist being strapped. This precautionary measure was prompted by the instability experienced during rowing by all three participants when their feet were not securely strapped.

Chapter 3 - Materials and Method

To ensure a comprehensive assessment, each study participant made two separate visits to our laboratory, with the time between these visits never exceeding one week.

During the first visit (day 1), participants underwent a comprehensive familiarization process with the ergometer, utilizing all four setups. This familiarity phase was essential to ensure that participants were comfortable with the equipment and procedures. Following the familiarization session, participants were instructed to engage in a rowing exercise for a continuous duration of 4 minutes at approximately the highest possible submaximal intensity within each setup. Between every setup, participants had a break of 2-5 minutes to avoid fatigue and its possible effect on the rowers' technique. It is important to note that the prescribed intensity was submaximal, indicating that participants were expected to rely solely on aerobic energy sources during rowing.

Throughout these sessions, we closely monitored three critical physiological parameters: heart rate, oxygen uptake (VO_2) and the Respiratory Exchange Ratio (RER). Heart rate was monitored using a H10 Polar heart rate monitor (Polar Electro Inc., Kempele, Finland). Rate of oxygen uptake (VO_2) was recorded using an ergospirometer with a mixing chamber (Oxycon Pro, Jaeger GmbH, Hoechberg, Germany) and a mouthpiece (Hans Rudolph Inc, Kansas City, MO, USA). Prior to testing, the gas analyzer was calibrated against a known mixture of gases (15% O_2 and 5% CO_2) and ambient air. These variables were instrumental in gauging the intensity and metabolic demands of rowing in each setup. The ergospirometer displays real-time physiological variables, such as the Respiratory Exchange Ratio (RER), which offered insights into metabolic substrate utilization during exercise. It is noteworthy that an RER value of less than 1 is indicative of an aerobic condition and submaximal intensity when close to 1. Consequently, the RER allowed us to continually guide participants on the necessity to adjust intensity levels, either increasing or decreasing, to maintain a submaximal intensity.

Chapter 3 - Materials and Method

Additionally, after each setup, participants were also asked to indicate a subjective rate of perceived exertion (RPE) on a 6-20 Borg scale [34]. Three values of RPE were asked, related to muscular, cardiac, and overall perceived exertion. Furthermore, key rowing parameters such as power output and time for 500 meters were collected using the RP3 Rowing app (RP3 Rowing).

The purpose of this initial day was to allow participant to familiarize with the setups and to identify the correct intensity for each of them, expressed as power output (Watt) and time for 500 meters (minutes), in order to row for 4 minutes in a submaximal intensity. More specifically, the submaximal intensity was defined as the power output that would result in a Respiratory Exchange Ratio (RER) close to 1, with a targeted range between 0.9 and 1.

The tested setups during the first day were administered in the following order for all the participants: Setup 1, Setup 2, Setup 3 and Setup 4. This specific order was chosen with the aim of ensuring that participants did not begin with an initial discomfort but rather progressively increased the level of constraint from one setup to the next.

Chapter 3 - Materials and Method

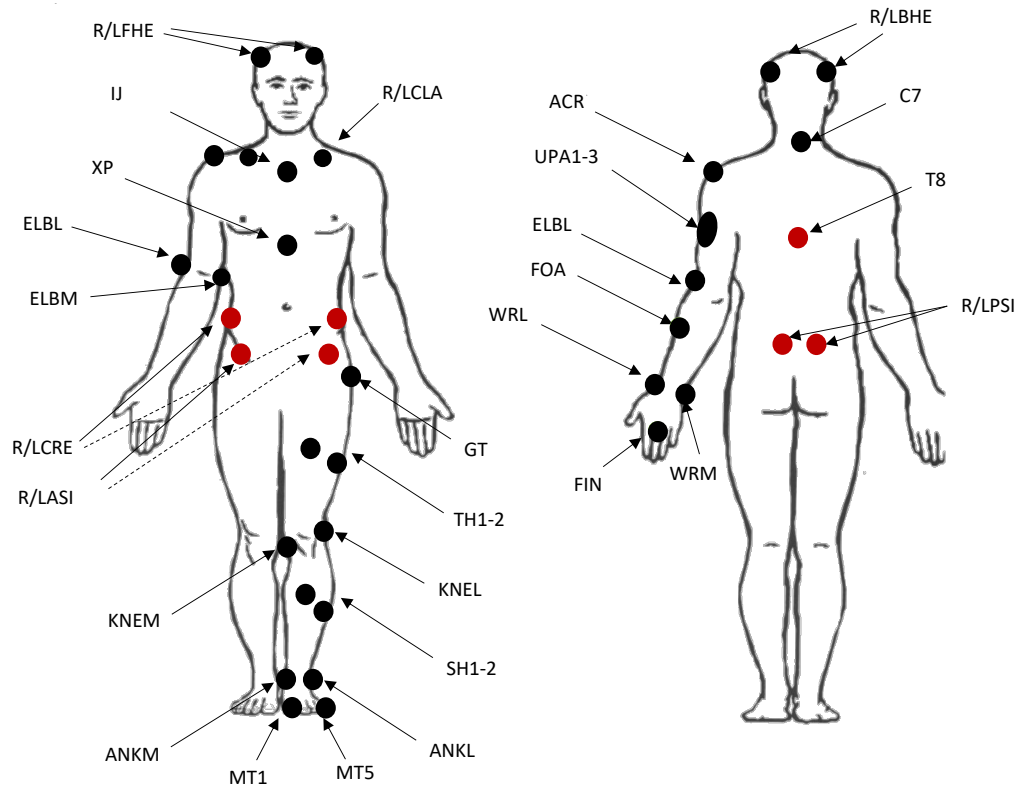


Figure 7 - Human body with markers' position. Each marker is identified by its respective label name. Notably, markers highlighted in red are exclusively present in setup 1 and setup 2.

On the second day of the testing protocol (day 2), each participant underwent specific procedures here described. At the beginning of the session, participants were weighed, electromyography sensors (Ambu BlueSensor, Ambu A/S, Ballerup, Denmark) were placed on the Latissimus dorsi, Trapezius, Rectus femoris, Biceps Brachii and Erector spinae muscles and retroreflective markers were placed on their body to collect the movement during the test using a motion capture software as Qualisys Track Manager (QTM, Qualisys AB, Gothenburg, Sweden). It was assumed that movement exhibited bilateral symmetry; thus, most of the markers were affixed only on the left side of the body using double-sided tape (3M Company in Minnesota, USA).

On the participant 37 retroreflective low-mass markers (14 mm in diameter) were allocated to the following anatomical landmarks (Figure 7 - Human body with markers' position). Each marker is identified by its respective label name. Notably, markers highlighted in red are exclusively

Chapter 3 - Materials and Method

present in setup 1 and setup 2.): four on the head (two positioned right front and right back, and two left front and left back), spinous process of the C7 and T8, Incisura Jugularis, Xiphoid process, bilaterally on the Clavicle, bilaterally on the posterior and anterior superior iliac spine, iliac crest, acromion process, lateral epicondyle of humerus, medial epicondyle of humerus, middle of forearm, lateral and medial wrist, 3rd finger knuckle, greater trochanter of femur, two markers in the middle of thigh segment, lateral and medial epicondyle of femur, two markers in the middle of the shank segment, lateral and medial malleolus, 1st and 5th metatarsal. In addition, a non-collinear cluster with three markers was attached to the lateral surface of the middle arm.

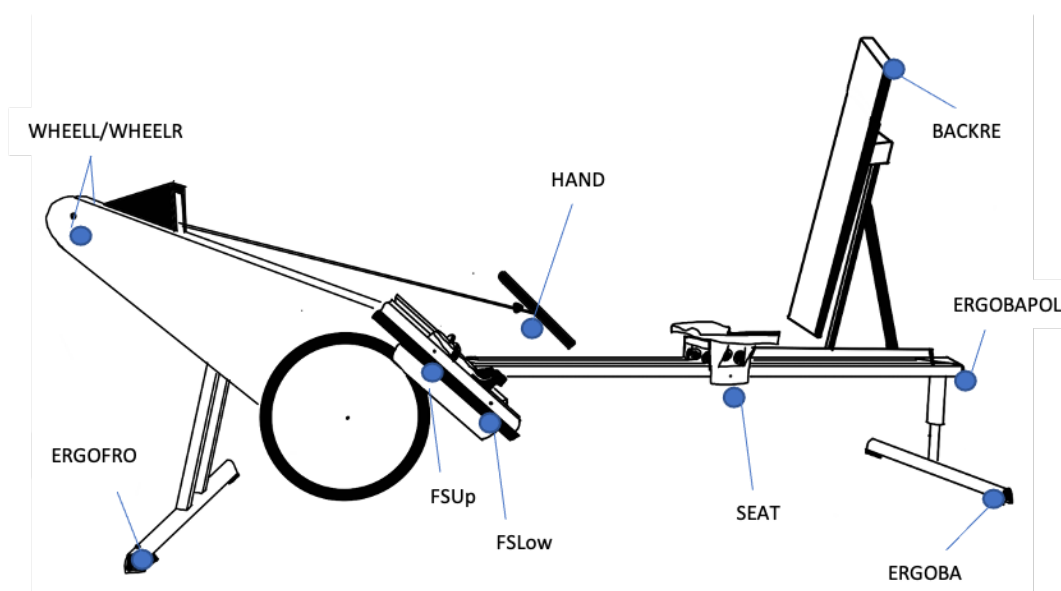


Figure 8 - Ergometer with markers' placement. Each marker is identified by its respective label name.

Ten markers were placed on the ergometer (Figure 8), particularly, one on the handle and one on the left side of the seat to record their movement, two on the foot stretcher, two on the flywheel, one on the back pole and two for the ergometer bases, one in front and one in the back, and one on the top of the backrest to record unintentional movements. As for the body, markers were fixed only on the left side assuming bilateral symmetry movement.

Chapter 3 - Materials and Method

The markers were placed by the same person throughout the data collection. Some markers, both on the ergometer and the participant, were excluded during specific protocol conditions. For instance, the marker on the backrest was exclusively utilized in setup 3 and setup 4 when the backrest was employed. Similarly, the marker on the back pole of the ergometer was visible only in setup 1 and setup 2, as the backrest covered it during the other setups. Furthermore, in setup 3 and setup 4, the markers on the posterior superior iliac spine, the markers on the anterior superior iliac spine and the ones on the iliac crest were removed due to the presence of the backrest and belts. For the same reason, the T8 marker was removed for setup 4.

Chapter 3 - Materials and Method

Table 3 - The table provides details on the body markers and on the markers applied on the ergometer, including their label names and corresponding position descriptions. Additionally, it contains information regarding the presence or absence of markers for various setups. In the table, a checkmark (✓) signifies that the marker is present during that setup, an "X" indicates the marker's absence, and "R" denotes that the marker position is reconstructed later using other markers as references.

Segment	Label name	Description	Setup			
			1	2	3	4
HEAD	RFH	Headband with 4 markers for head: front right	✓			
	RBH	Headband with 4 markers for head: back right	✓			
	LFH	Headband with 4 markers for head: front left	✓			
	LBH	Headband with 4 markers for head: back left	✓			
TRUNK	C7	Over the spinous process of the 7th cervical vertebrae	✓			
	T8	Over the spinous process of the 8th thoracic vertebrae	✓			R
	IJ	On the Incisura Jugularis	✓			
	XP	On the Xiphoid process	✓			
	RCLA	Right shaft of clavicle	✓			
	LCLA	Left shaft of clavicle	✓			
PELVIS	RPSI	Right Posterior superior iliac spine	✓			X
	LPSI	Left Posterior superior iliac spine	✓			X
	RASI	Right anterior superior iliac spine	✓			X
	LASI	Left anterior superior iliac spine	✓			X
	RCRE	Right Top of Iliac crest	✓			X
	LCRE	Left top of iliac crest	✓			X
ARM	ACR	Acromion process	✓			
	UPA 1-3	Cluster of 3 markers, middle of arm	✓			
	ELBL	lateral epicondyle of humerus	✓			
	ELBM	medial epicondyle of humerus	✓			
FOREARM	FOA	middle of forearm	✓			
	WRL	lateral wrist	✓			
	WRM	medial wrist	✓			
HAND	FIN	knuckle of 3 rd finger	✓			
THIGH	GT	greater trochanter of femur	✓			
	TH1	marker on middle of the anterior thigh segment (proximal to TH2)	✓			
	TH2	marker on middle of the anterior thigh segment (distal to TH1)	✓			
	KNEL	lateral epicondyle of femur	✓			
	KNEM	medial epicondyle of femur	✓			
SHANK	SH1	marker on middle of the anterior shank segment (proximal to SH2)	✓			
	SH2	marker on middle of the anterior shank segment (distal to SH1)	✓			
	ANKL	lateral malleolus	✓			
	ANKM	medial malleolus	✓			
FOOT	MT1	base of 1st metatarsal	✓			
	MT2	base of 5th metatarsal	✓			
ERGOMETER	HAND	In the middle of the handle, positioned on the connection point with the chain	✓			
	SEAT	Left side of the seat	✓			
	FSUp	Left side of the foot-stretcher proximal to FSLow	✓			
	FSLow	Left side of the foot-stretcher distal to FSUp	✓			
	WHEELL	Flywheel, left side	✓			
	WHEELR	Flywheel, right side	✓			
	ERGOFRO	Ergometer front base, on the left side	✓			
	ERGOBA	Ergometer back base, on the left side	✓			
	ERGOBAPOL	Ergometer back pole	✓			X
	BACKRE	Top of the backrest	X			✓

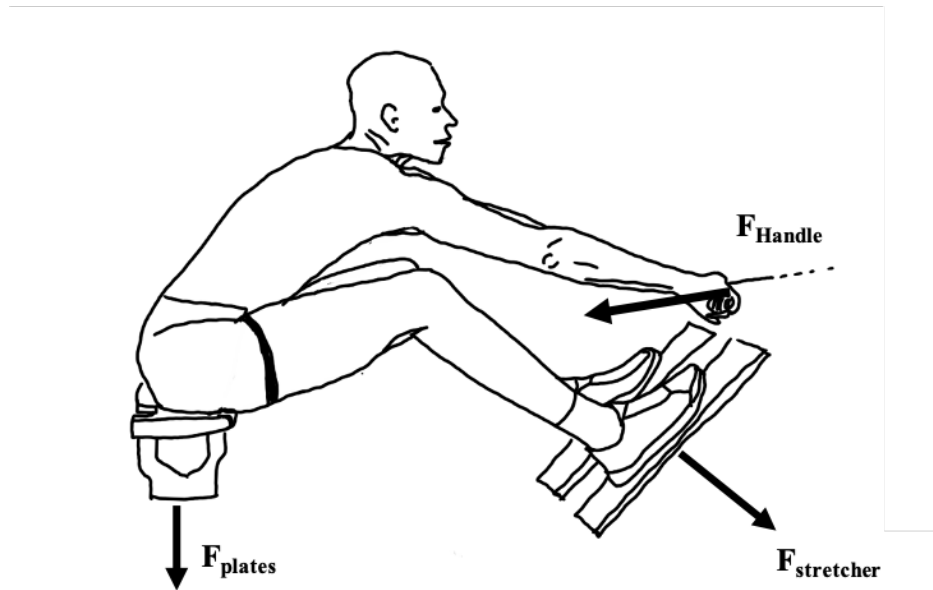


Figure 9 - Free body diagram of the rower with the external forces

The ergometer was instrumented to measure external forces applied on the handle, the foot-stretcher and the seat. In the free body diagram is presented the rower and the external forces applied (Figure 9). The ergometer was placed on two force plates (Kistler 9286 BA, Kistler Instruments AG, Winterthur, Switzerland), one for each support base to measure the forces at the seat F_{plates} . One of the stretchers was equipped with a custom-made force plate existing of three 3D Kistler force cells (Kistler Instruments AG, Winterthur, Switzerland) to measure the force at the foot-stretcher $F_{\text{stretcher}}$. Both the $F_{\text{stretcher}}$ and F_{plates} were sampled at 200 Hz. To record the handle force F_{Handle} , between the handle and the chain was positioned a uniaxial load cell (N-DTS-FS5, Noraxon USA Inc., Scottsdale, Arizona), sampled at 1500 Hz.

3.3.2 Collection

At the beginning of each session, the optical system was calibrated, using a wand and L-frame (Qualisys AB, Gothenburg, Sweden). Before each test session, a static trail was conducted to establish a personalized kinematic reference model for each participant. During this trial, the participant stood

Chapter 3 - Materials and Method

in the anatomical neutral position standing beside the left side of the ergometer or sitting on a box in the same place. All kinematic data was acquired using eleven infrared Oqus cameras (Qualisys AB, Gothenburg, Sweden), capturing at 100 Hz.

Following this, participants engaged in a 10 minutes warm-up routine, after which they were equipped with both a heart rate sensor and a mouthpiece for monitoring VO₂ uptake as in the first day of protocol.

The sequencing of the second day's testing protocol commenced with the ergometer configured in Setup 4; subsequently, the sequence progressed from Setup 4 to Setup 3, then to Setup 2 and finally to Setup 1. The selection of this order, reversed from day 1, was made primarily for ergonomic convenience when adjusting the ergometer settings. Additionally, since the rowing sessions were designed to maintain submaximal intensity with an RER < 1, and with appropriate rest periods between setups to prevent the accumulation of fatigue, there was no need for randomization in the order of the setups.

Within each setup, participants were instructed to row for a duration of precisely 4 minutes while maintaining a given power output established during their initial day in the laboratory. This intensity was quantified in Watts and corresponded to the average Power produced during the day one session. Notably, as participants engaged in rowing, they had access to real-time feedback as power output (watts), split (i.e., time for 500 meters, minutes) and time (hh:mm:ss), displayed on the phone's screen using the application RP3 Rowing Lite (RP3Rowing Bv., The Netherlands). As in the first day of protocol, between each setup, participants had a time break of 2-5 minutes to avoid fatigue and its possible effects on rowing technique.

During Day 2, for every setup, motion data was captured throughout the entire 4-minute duration, employing motion capture software Qualisys Track Manager (QTM; Qualisys AB, Gothenburg, Sweden).

On the second day of data collection, from force sensors placed under the ergometer, on one foot-stretcher and between the chain and the handle, we gathered additional information which were employed for the purpose of

conducting kinetic analysis. Similar to the procedures followed on the first day of data collection, each participant was asked to provide ratings on a 6-20 Borg scale [34] for three specific aspects: muscle intensity, cardiac intensity and overall perceived exertion, following each setup. Moreover, during the second day of measurements, following each setup, the participant's lactate levels from their fingertip was measured. This contributed to verify that across setups there were not accumulation of fatigue.

Respiratory data and heart rate are used only to determine the right intensity during the first day of protocol, due to this reason, these data will not be presented.

3.4 Data Processing

3.4.1 QTM

From the recording with kinematic, kinetic and EMG synchronized measurements, a segment of 40-second interval from the middle of the recording was extracted. This was subjected to an analysis to ensure the consistency of the captured activity.

All markers were systematically associated to unique labels, as detailed in Table 3. Subsequently, the trajectory of each marker underwent a visual examination, with particular attention to identifying and addressing any potential gaps. These gaps were filled through software operations based on the trajectories of other markers positioned on the same body segment. The QTM software allowed to use various techniques depending on the gap size. For smaller gaps, it connected the gap's extremity with a polyline, while for larger gaps, it generated the missing coordinates by extrapolating from the coordinates of nearby markers decided by user.

Once this process is completed, and all markers have been accurately labeled and any gaps resolved, the data is exported into a .mat file format for subsequent analysis using the MATLAB (9.10.0 R2021a, MathWorks Inc., Natick, MA, USA) software.

Chapter 3 - Materials and Method

It is worth noting that, on occasion, certain markers were not captured during measurements, likely due to partial obstructions caused by other body parts or the ergometer during movement. Additionally, in setup 4, the T8 marker was not utilized because of the presence of the backrest. In such instances, we employed MATLAB to reconstruct the missing markers data based on their positions during the static trial and the position of the nearby markers during the recording.

The .mat file imported into MATLAB contains both kinematic and kinetic data. Both datasets have undergone a filtering process using a dual-pass 2nd order Butterworth filter with an 8 Hz cut-off frequency. This filtering procedure was implemented to enhance data quality by removing unwanted noise, rendering the data ready for subsequent analysis.

3.4.2 Biomechanical model

The body is considered to be comprised of rigid segments analyzed within a three-dimensional framework. Specifically, the definition the biomechanical model is subject to variation, depending on the particular setup under examination, which in turn influence markers' position.

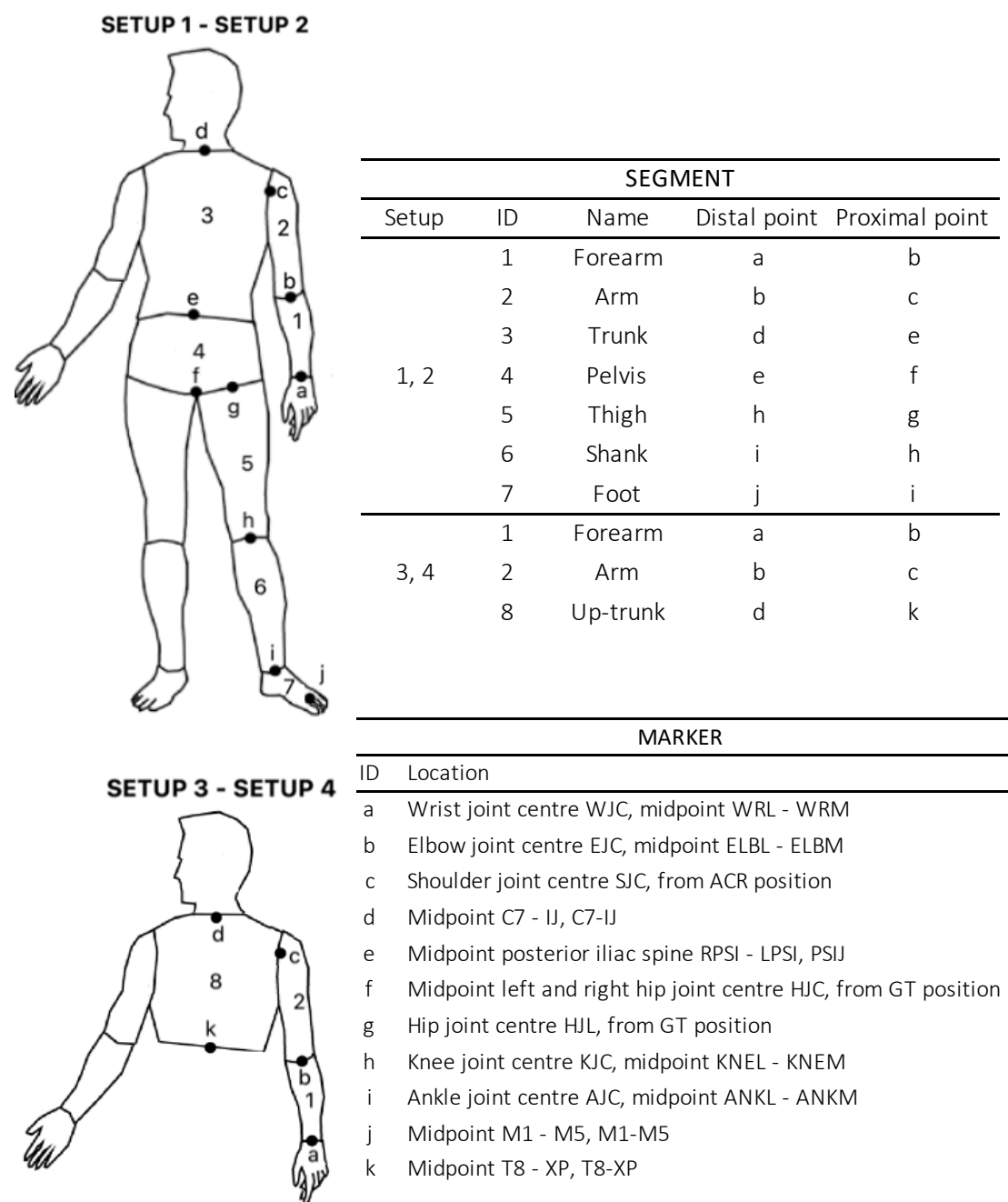


Figure 10 - Segment definition distinct based on the setup. Illustration with segment ID and marker ID, tables with segment and markers explanation.

Chapter 3 - Materials and Method

In setup 1 and setup 2, participants row on the ergometer with their feet placed in the foot-stretchers and without the presence of the backrest. So, all the markers on the pelvis are visible and even the T8 marker. Due to this, the body segments as forearm, arm, trunk, pelvis, thigh, shank, and foot were defined. Instead, in setup 3 and setup 4, due to the presence of the backrest, the markers on the pelvis are not positioned and the lower part of the body is not moving, so for these reasons the body segments as forearm, arm, and up-trunk were defined.

The distinction between the trunk segment and the up-trunk segment lies in the markers that delineate them. Specifically, the trunk segment is defined as the region between the midpoint situated between the C7 and IJ markers and the midpoint between the markers on the pelvis, namely RPSI and LPSI. In contrast, the up-trunk segment encompasses the space between the midpoint of the C7 and IJ markers and the midpoint between the T8 and XP markers. However, despite the use of two distinct segments to describe torso movement across the setups, the presence of movement constraints in setup 3 and setup 4 renders the up-trunk segment sufficient to understand the movement.

Figure 10 - Segment definition distinct based on the setup. Illustration with segment ID and marker ID, tables with segment and markers explanation. provides a comprehensive overview of the multibody model. It shows also the markers used for the definition of the segments as their proximal and distal points, and the setups in which they are employed.

It's essential to highlight that the choice of the multibody model influences the outcomes of the study [35].

In the case of certain segments, the definition necessitates establishing the center of connective joints. For instance, defining the arm segment requires determining the center of rotation of the shoulder joint (SJC) as its proximal point. This calculation relies on the spatial position of the acromion marker (ACR), following the methodology outlined by H.E.J. Veeger, et.al [36]. Particularly, H.E.J. Veeger, et.al, established that the centre of rotation of the shoulder joint can be calculated as the center of a sphere through the glenoid surface, with the radius of the humeral head. The estimated shoulder

joint center is positioned 9.7 mm medial, 32.0 mm proximal, and 25.9 mm posterior from the ACR position.

Additionally, defining the pelvis and thigh segments involves establishing the hip joint center (HJL). This is determined based on the position of the great trochanter (GT) marker, adhering to established guidelines by T. Joshua, et.al [38]. Notably, using the GT position yields to estimate the HJC as 7.6 mm medial, 12.2 mm posterior, and 4.8 mm proximal from the GT.

3.4.3 Coordinate system definition

For the biomechanics analysis and for an easier comprehension of the system, a convention or coordinate system is required. Employing an inertial coordinate system (ICS) enables us to express segment information within a nonaccelerating system in which Newton's laws of motion are valid [37-39].

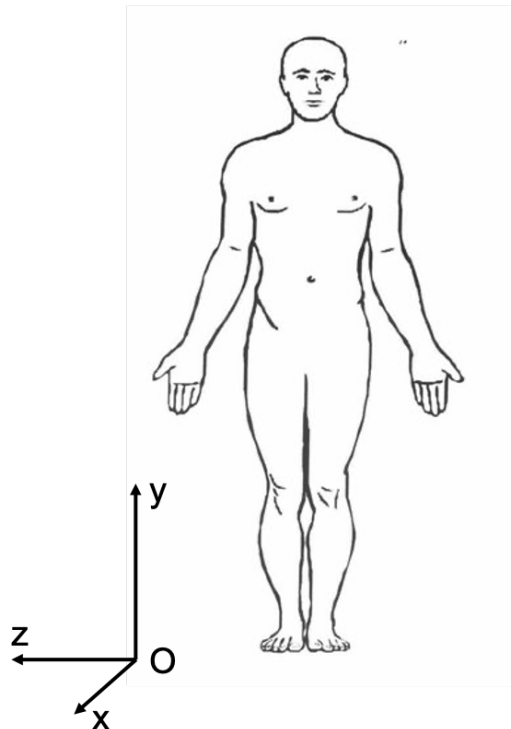


Figure 11 - Inertial Coordinate System (ICS).

For this study, the ICS has been defined with the axis orientation as in Figure 11 where X-axis defines the anterior – posterior direction (i.e., +ive X is anterior), Y-axis defines the vertical direction (i.e., +ive Y is pointing up)

Chapter 3 - Materials and Method

and Z-axis defines the medio-lateral direction (i.e., +ive Z is pointing right). The origin of the ICS is positioned on the ground and, as its orientation, it is considered stationary for the all study.

However, in human movement analysis it is often more interesting to express movements of segments in relation to other segments, for example joint angles. Terms such as proximal/distal, flexion/extension, abduction/adduction and rotation are a defined convention established by the anatomical literature that allows to describe the movement [40-42].

As a result, it is possible to establish segment coordinate systems, known as Local Coordinate Systems (LCS), by utilizing the positions of markers. This process relies on information from the existing literature, and specifically adheres to the ISB recommendations [43, 44].

From Figure 12 to Figure 18 there is a provided visual representation of the segments along with the associated local coordinate systems, while the presented tables list the markers used to define the axes.

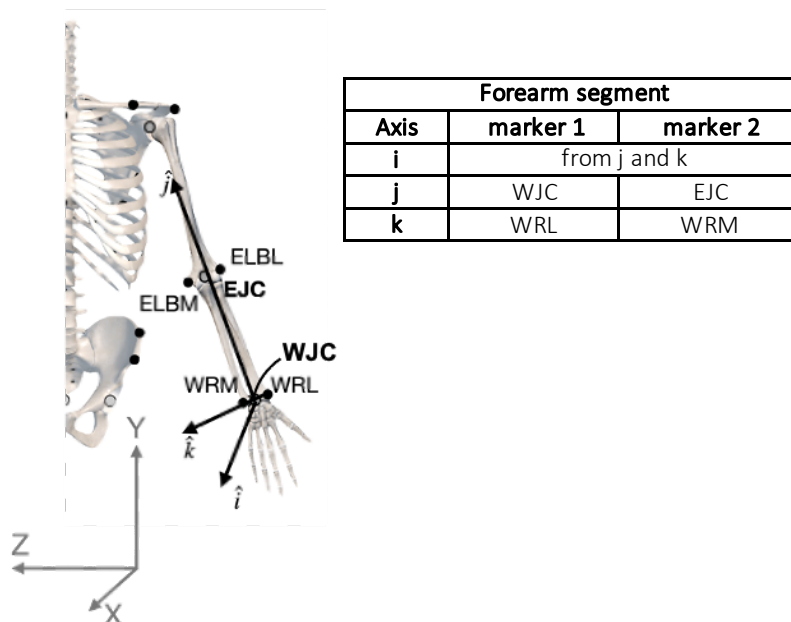


Figure 12 - Forearm segment LCS. Anterior view of the forearm and arm. Axis of the forearm LCS (Local Coordinate System) and the placement of markers.

Chapter 3 - Materials and Method

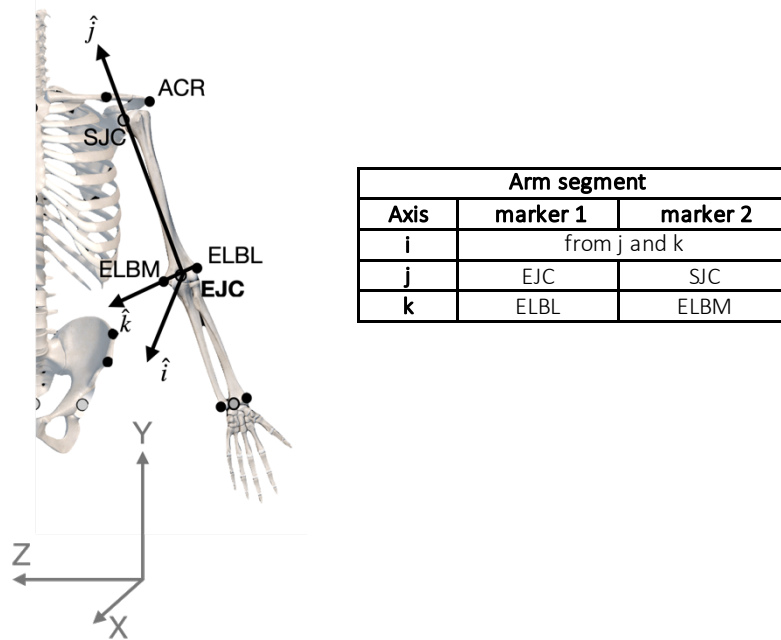


Figure 14– Arm segment LCS. Anterior view of the forearm and arm. Axis of the arm LCS (Local Coordinate System) and the placement of markers

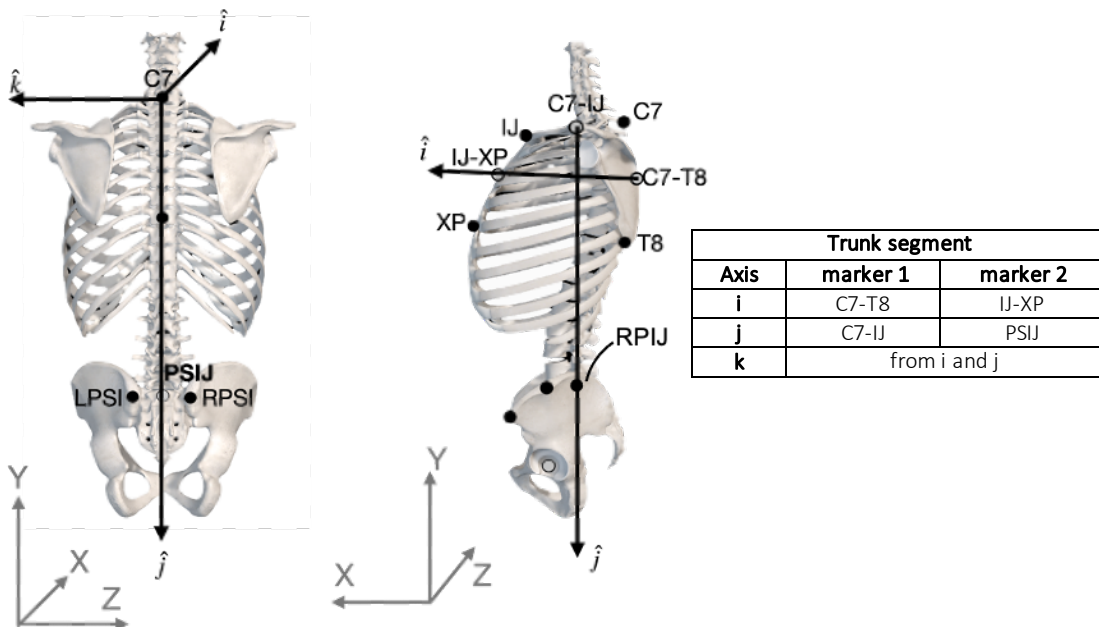


Figure 13 - Trunk segment LCS. Posterior and the left side view of the trunk and pelvis. Axis of the trunk LCS (Local Coordinate System) and the placement of markers.

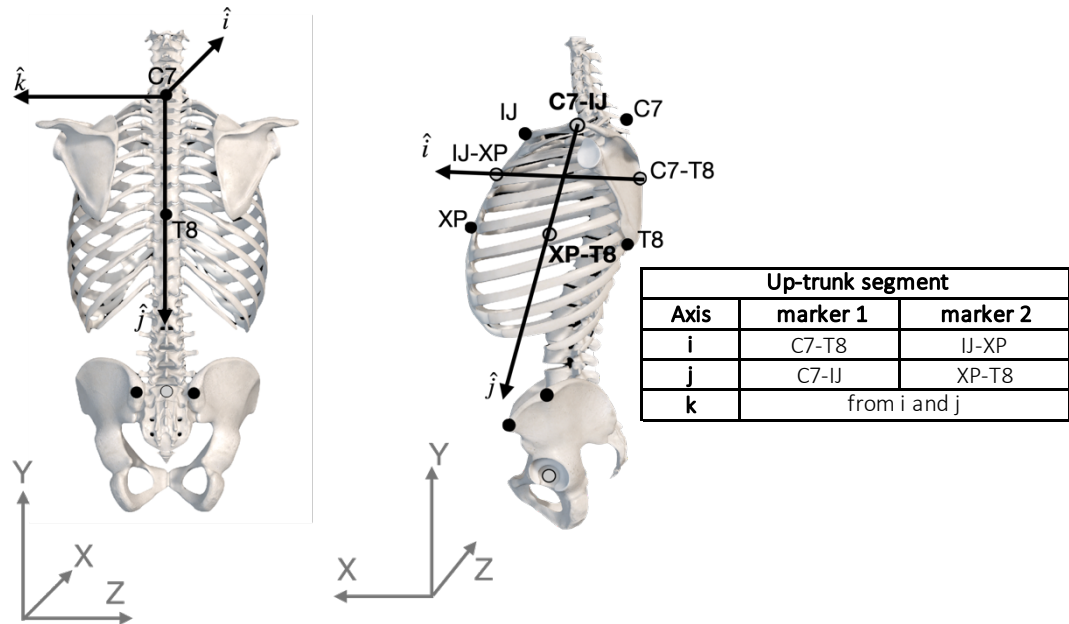


Figure 15 - Up-trunk segment LCS. Posterior and the left side view of the trunk and pelvis. Axis of the up-trunk LCS (Local Coordinate System) and the placement of markers.

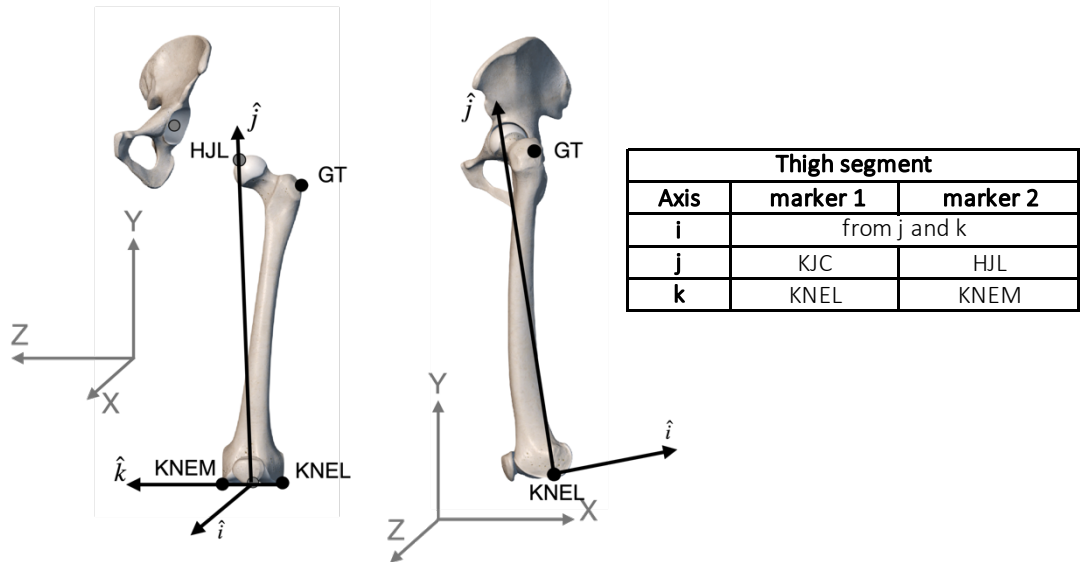


Figure 16 -Thigh segment LCS. Anterior and the left side view of the thigh. Axis of the thigh LCS (Local Coordinate System) and the placement of markers.

Chapter 3 - Materials and Method

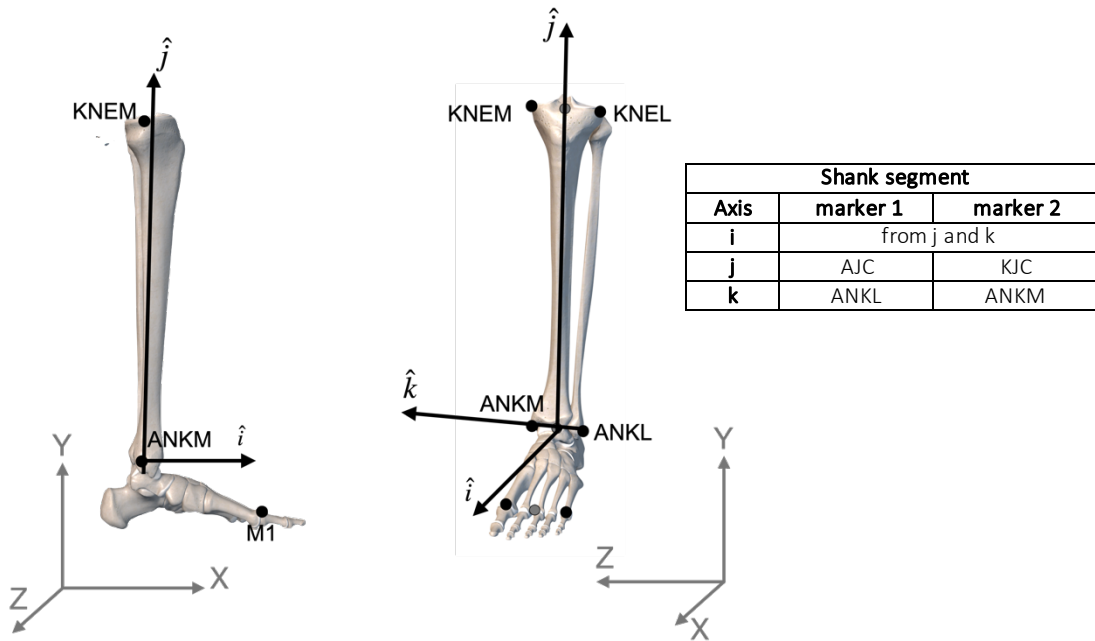


Figure 17 - Shank segment LCS. Medial and the anterior view of the shank and foot. Axis of the shank LCS (Local Coordinate System) and the placement of markers.

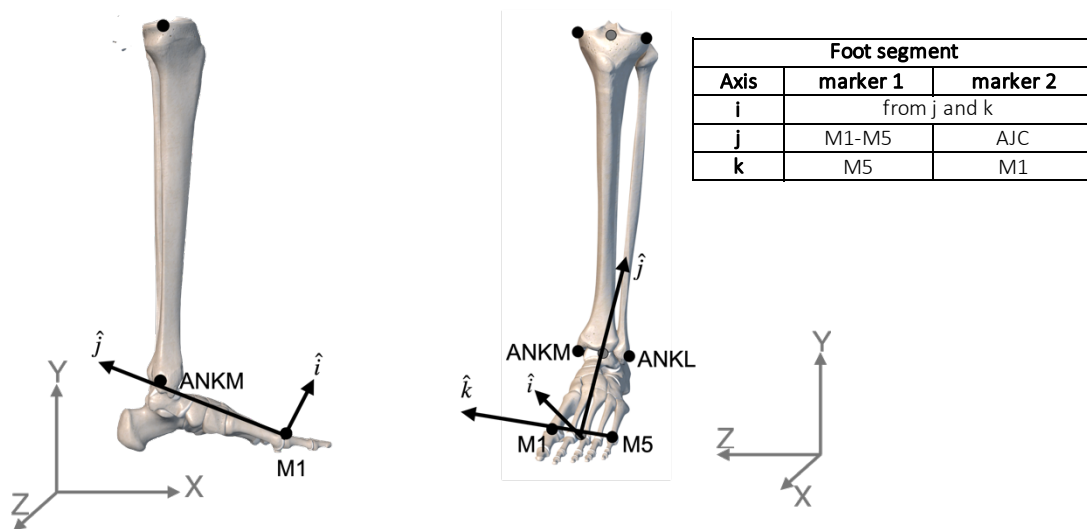


Figure 18 - Foot segment LCS. Medial and anterior view of the shank and foot. Axis of the foot LCS (Local Coordinate System) and the placement of markers.

To express the position of a point in the LCS of the proximal one, we define a rotation matrix R . This matrix allows to express the coordinate of the point from the ICS to the LCS of another segment as in (1) .

$$\begin{bmatrix} x \\ y \\ z \end{bmatrix}^{LCS} = {}^{ICS}[R]_{LCS} \cdot \begin{bmatrix} x \\ y \\ z \end{bmatrix}^{ICS} \quad (1)$$

Where $\begin{bmatrix} x \\ y \\ z \end{bmatrix}^{LCS}$ are the coordinate in the LCS
 $\begin{bmatrix} x \\ y \\ z \end{bmatrix}^{ICS}$ are the coordinate in the ICS
 ${}^{ICS}[R]_{LCS}$ is the rotation matrix from ICS to LCS

3.4.4 Joint definition

We define joint as the connection between two segments. As for the segment definition, the joint definition depends on the setup under analysis. Particularly, for the setup 1 and 2, when the body is considered in its entirety, the joint are:

- Elbow joint: between forearm and arm
- Shoulder joint: between arm and trunk
- L5-S1 joint: between trunk and pelvis
- Hip joint: between pelvis and thigh
- Knee joint: between thigh and shank
- Ankle joint: between shank and foot

Instead, for the setup 3 and setup 4 where we consider only the upper part of the body, the joints are defined as:

- Elbow joint: between forearm and arm
- Shoulder joint: between arm and up-trunk
- T8 joint: between up-trunk and inertia coordinate system

In this study we consider that all these joints exclusively permit rotational movements. Some of them allow rotation around all three axes, classifying them as joints with 3 degrees of freedom (3-DOF), while others allow

Chapter 3 - Materials and Method

rotation only around two axes, categorizing them as joints with 2 degrees of freedom (2-DOF).

With the exception of the elbow and knee joints, which are considered as 2-DOF, all the other joints are classified as 3-DOF.

For a detailed breakdown of the rotational axes and their corresponding anatomical movements, refer to Table 5.

JOINT DEFINITION	SEGMENTS CONNECTED		DEGREE OF FREEDOM
	distal	proximal	
Elbow	forearm	arm	2
Shoulder	arm	trunk /up-trunk	3
L5-S1 joint	pelvis	trunk	3
T8 joint	pelvis	up-trunk	3
Hip	thigh	pelvis	3
Knee	shank	thigh	2
Ankle	foot	shank	3

Table 4 – A comprehensive overview of joint definitions, emphasizing the segments associated with each joint and the Degrees of Freedom (DOF) for each joint.

JOINT	ROTATION AXIS NAMES		
	Rotation axis x (i)	Rotation axis y (j)	Rotation axis z (k)
Elbow	-	pronation (+) / supination (-)	flexion (+) / extension (-)
Shoulder	adduction (+) / abduction (-)	medial (+) / lateral (-) rotation	flexion (+) / extension (-)
L5-S1 joint	lateral trunk flexion right (+) / left (-)	right (+) / left (-) rotation	flexion (+) / extension (-)
T8 joint	lateral trunk flexion right (+) / left (-)	right (+) / left (-) rotation	flexion (+) / extension (-)
Hip	lateral pelvis flexion right (+) / left (-)	right (+) / left (-) rotation	flexion (+) / extension (-)
Thigh	adduction (+) / abduction (-)	medial (+) / lateral (-) rotation	flexion (+) / extension (-)
Knee	-	medial (+) / lateral (-) rotation	flexion (+) / extension (-)
Ankle	inversion (+) / eversion (-)	medial (+) / lateral (-) rotation	dorsiflexion (+) / plantarflexion (-)

Table 5 - Rotation axis names for each joint. These are presented in the Local Coordinate System (LCS) of the proximal segment for reference.

3.4.5 Time-normalization and statistics

In our study, we adopted the convention to define a rowing cycle as the interval between two consecutive catch events. Specifically, to establish the catch event, the position of the marker on the handle is used. The catch event was determined as the handle's position closest to the flywheel, while the finish event was identified as the handle's position farthest from the flywheel.

Each variable under analysis was time-normalized, facilitating a meaningful comparison among participants and setups. Specifically, time normalization involved resampling each variable to consist of 100 samples, covering the entire rowing cycle time from 0% to 100%. Following time normalization, variables were averaged across cycles to obtain an average cycle, and the standard deviation around cycles was also calculated. For the AB group, the variable values for all participants were averaged to derive a group variable along with its standard deviation. This approach allowed us to make meaningful comparisons and assess the consistency of variables across participants and setups.

All data were stored offline and processed in MATLAB. Data are presented as means \pm standard deviation (SD).

In each analysis participants from the AB group are considered as a group while participants with physical impairments are considered individually and compared with the AB group.

3.4.6 Stroke rate, Stroke length and Drive phase duration

From the motion capture data, it is possible to extract some variables. The Stroke rate (SR) is defined as the number of rowing cycles executed per minute and is expressed in units of strokes per minute [$\text{strokes} \cdot \text{min}^{-1}$]. The Stroke length (LS) is determined by measuring the difference in the handle's coordinates between the catch and finish events and is expressed in meters [m]. The drive phase duration [%] is defined as the time between the

initiation of a rowing cycle (catch event) and the conclusion of the driving phase (finish event).

3.4.7 Kinematic data processing

The kinematic analysis is an integral aspect of this study, focusing on the range of motion (ROM) exhibited by various body segments. To achieve a comprehensive understanding of this motion, it becomes imperative to establish reference points and directional criteria, as outlined by previous research [45]

In our kinematic analysis, we consistently define the ROM of each segment in relation to its proximal counterpart. This approach allows us to calculate the relative angles between segments, effectively characterizing joint angles. However, certain segments, such as the trunk, up-trunk, and thigh, are expressed in relation to the Inertial Coordinate System (ICS) for enhanced clarity and comprehension. A detailed overview of these segments, along with the corresponding coordinate systems for expressing angles, is conveniently provided in Table 6.

ANGLE NAME CONVENTION		
Expressed segment	in LCS of	Angle name
Forearm	Arm	Elbow
Arm	Trunk/Up-trunk	Shoulder
Trunk / Up-trunk	ICS	Trunk
Pelvis	ICS	Pelvis
Thigh	ICS	Thigh
Shank	Thigh	Knee
Foot	Shank	Ankle

Table 6 - Nomenclature convention employed to denote the angles of the body segments based on the Local Coordinate System (LCS) used for their expression.

It is essential to note that when expressing these joint angles, we meticulously account for the degrees of freedom permitted by the specific joint under examination. This approach ensures that our analysis accurately reflects the biomechanical intricacies of the human body's movements. Table 5 offers insight into the positive angle conventions applied to the analyzed

angles. Furthermore, the establishment of a zero reference point for each angle is of paramount importance. In the context of our study, these angles are defined with a zero reference when the body is in its natural anatomical position. This zero reference point acts as the foundation for consistent and standardized angle measurements, underpinning the accuracy and reliability of our biomechanical analysis.

The evaluation of the segment's angles, needs the definition of the sequence of rotation in a way to describe uniquely the movement. In fact, it is important to report the choice of rotation sequence since different sequences may yield different angles [35, 45-47]. In this project the sequence of rotation is defined as "ZXY" that means the principal rotation of the joints is expected to be around the medial-lateral axis (Z-axis), thus, flexion – extension rotation.

In addition to the angles discussed in our kinematic analysis, there are several other essential variables that play a fundamental role in completing the kinetic analysis. Specifically, it is crucial to define the linear velocity and linear acceleration of various key points, including the distal and proximal points, as well as the center of mass (COM) for each segment. Additionally, the angular velocity and angular acceleration are vital components of this analysis.

The derivation of these variables involves computing the changes in position (x, y, z) over time, leading to the calculation of velocity ($\dot{x}, \dot{y}, \dot{z}$). To determine the angular variables, we multiply the derivatives by the unit vectors associated with the three rotation axes: Z, X, and Y. This process is elaborated in the Equation below:

$$\omega = B(\theta, \psi) \begin{bmatrix} \dot{\phi} \\ \dot{\theta} \\ \dot{\psi} \end{bmatrix} \quad (2)$$

Here, φ represents the rotation angle around the Z axis, θ corresponds to the rotation angle around the X axis, and ψ signifies the rotation angle around the Y axis. Furthermore, the matrix B is defined as illustrated in Equation (3).

$$B(\theta, \psi) = \begin{pmatrix} -\cos(\theta) \sin(\psi) & \cos(\psi) & 0 \\ \sin(\theta) & 0 & 1 \\ \cos(\theta) \cos(\psi) & \sin(\psi) & 0 \end{pmatrix} \quad (3)$$

These variables serve as critical components in our subsequent kinetic analysis.

3.4.8 Kinetic data processing

To analyze the power generated by the joints under examination, we employed the Inverse Dynamic approach.

The 3d Inverse dynamic was implemented using MATLAB and drew upon the methodologies outlined in several prior studies, such as [48-53].

To provide a clearer understanding, the Inverse Dynamic analysis begins by considering a distal segment, for which we have information about external moments and forces. We apply Newton's equations of motion to this segment, allowing us to estimate previously unknown joint forces and moments for the proximal segment. These joint forces and moments are then used to solve Newton's equations for the next, more proximal segment, thereby enabling the determination of forces and moments at the adjacent joint.

SETUP 1-2		
Chain	Joint	Application point of the distal forces
1	Elbow Shoulder L5-S1 joint	Handle Elbow Shoulder
2	Ankle Knee Hip	Foot-stretcher Ankle Knee

SETUP 3-4		
Chain	Joint	Application point of the distal forces
1	Elbow Shoulder T8 joint	Handle Elbow Shoulder

Table 7 – This table illustrates the two analyzed chains used for power calculations in the joints. It provides details on the point of application of distal forces used for force and power calculations in each joint, while also highlighting variations across different setups.

We calculated inverse dynamic by dividing the body model into two distinct chains. Specifically, for the upper body, we applied the external force from the handle (F_{Handle}) on the forearm, and the chain extended from the forearm segment to the trunk segment. For the lower body, we used the external force from the foot-stretcher ($F_{\text{Stretcher}}$), with the chain spanning from the foot to the pelvis segments. Table 7 provides an overview of the analyzed chains, emphasizing the joints encompassed in each.

It's worth noting that in setups 1 and 2, we considered both chains, while in setups 3 and 4, only the upper chain was taken into account.

The parameters used for the Inverse Dynamic analysis, as moment of inertia, mass and centre of mass of the segments, were estimate applying the equations based on anthropometric data according to de Leva [54, 55], segments' length and individual body mass. Particularly, the segments' length is calculated as the difference between the proximal and distal points.

Chapter 3 - Materials and Method

SEGMENT	MASS (%)		Longitudinal COM position (%)		RADII OF GYRATION (%)					
	M	F	M	F	Saggital		Longitudinal		Transverse	
					M	F	M	F	M	F
Forearm	2.3	1.94	45.74	45.59	27.6	26.1	12.1	9.4	26.5	25.7
Arm	2.71	2.55	42.58	57.54	28.5	27.8	15.8	14.8	26.9	26
Trunk + Head	32.29 + 6.94	30.1 + 6.68	44.86	44.86	37.2	35.7	19.1	17.1	34.7	33.9
Up-trunk + Head	15.96 + 6.94	15.45 + 6.68	29.99	20.77	71.6	74.6	65.9	71.8	45.4	50.2
Pelvis	11.17	12.47	61.15	49.2	61.5	43.3	58.7	44.4	55.1	40.2
Thigh	14.16	14.78	40.95	36.12	32.9	36.9	14.9	16.2	32.9	36.4
Shank	4.33	4.81	44.59	44.16	25.5	27.1	10.3	9.3	24.9	26.7
Foot	1.37	1.29	44.15	40.14	25.7	29.9	12.4	13.9	24.5	27.9

Table 8 – Anthropometric measures from P. De Leva (1996). Mass is the mass (%) of the segment relative to the body mass; Longitudinal COM position and radii of gyration are both relative to the respective segment length.

The inverse dynamic approach involves estimating the net joint moments, which, when multiplied with joint angular velocity, provide the joint power.

$$Power = Moment \cdot \omega \quad (4)$$

Where ω is the angular velocity of the joint.

Handle power (P_{handle}) is calculated as F_{handle} multiplied by the handle's velocity.

$$P_{handle} = F_{handle} \cdot v_{handle} \quad (5)$$

The total body mechanical energy (E_{body}) is calculated as the sum of the total energy of all segments:

$$E_{body} = \sum_{i=1}^n E_i \quad (6)$$

Where

$$\begin{pmatrix} n = 6 \text{ if Setup 1, Setup 2} \\ n = 3 \text{ if Setup 3, Setup 4} \end{pmatrix}$$

Chapter 3 - Materials and Method

Where E_i is the total energy of the segment i calculated as:

$$E_i = E_{potential} + E_{kinetic} \quad (7)$$

$$E_i = m_i \cdot g \cdot h_i + \frac{1}{2} \cdot m_i \cdot v_i^2 + \frac{1}{2} \cdot I_i \cdot \omega_i^2 \quad (8)$$

Where m_i is the segment mass [kg], g is the gravitational acceleration [$-9.81 m \cdot s^{-2}$], h_i is the segment height variation from the ground [m], v_i is the velocity of the segment expressed in the ICS [$m \cdot s^{-1}$], I_i is the moment of inertia of the segment [$kg \cdot m^2$] and ω_i is the angular velocity of the segment i expressed in the ICS [$rad \cdot s^{-1}$].

The total power generated by the rower, P_{rower} , is calculated as the sum of P_{handle} and the rate of change in time of E_{body} .

According to the power equation of Ingen Sechnau and Cavanagh (1990) [56], P_{rower} conceptually coincides also with the sum of the power generated in each joint, J_{sum} . Particularly the power in each joint is composed by the power in the three directions, as Px, Py and Pz for most of the joints.

$$P_{rower} = P_{handle} + \frac{dE_{body}}{dt} \quad (9)$$

$$J_{sum} = \sum_{i=1}^n P_i \quad (10)$$

Where $\begin{pmatrix} n = 6 \text{ if Setup 1, Setup 2} \\ n = 3 \text{ if Setup 3, Setup 4} \end{pmatrix}$

Where P_i is the summed power of the joint i , that is $P_x + P_y + P_z$.

Chapter 4

Results and Discussion

In the following graphs, participants in the AB group are uniformly represented in gray, providing a comprehensive view of the group's collective performance, while the mean value is presented in black. Conversely, individuals with physical impairments are individually presented, each with a distinct color as specified in the legend. Participants with physical impairments are denoted in the legend as PartA, PartB, and PartC, with "Part" indicating "Participant" and "A," "B," or "C" corresponding to their unique participant IDs assigned in Chapter 3.

Participants with physical impairments did not perform in all the four setups. Particularly, Participant A performed in setup 2, setup 3 and setup 4, while Participant B and Participant C performed only in setup 3 and setup 4 because of their physical impairments.

Chapter 4 - Results and Discussion

	Distance [m]	Mean Power Output [W]	Time/500m [min]	HR [bpm]	Bla [mmol/L]	RER	Peak Handle Force [N]	Drive Phase duration [%]	Stroke rate [spm]	Stroke length [cm]	P _{ower} [W]
Ab group	1	923.2 ± 110.4	02:13	159 ± 18	3.9 ± 2.7	0.90 ± 0.09	493.4 ± 143.4	25.5 ± 2.8	29.2 ± 0.7	138.5 ± 4.3	161.9 ± 52.9
	2	806.4 ± 116.5	02:34	146 ± 20	3.4 ± 1.5	0.91 ± 0.07	338.0 ± 114.5	23.1 ± 2.4	35.8 ± 1.3	102.8 ± 2.1	111.5 ± 40.6
	3	713.8 ± 102.8	02:55	136 ± 20	4.2 ± 2.0	0.96 ± 0.10	269.9 ± 98.3	21.8 ± 3.3	39.5 ± 2.5	80.0 ± 2.1	77.8 ± 30.8
	4	618.6 ± 82.2	03:21	132 ± 21	6.0 ± 2.8	1.06 ± 0.11	219.8 ± 64.5	20.8 ± 2.8	49.9 ± 2.3	51.6 ± 1.3	51.1 ± 16.8
PartA setup	2	741.5	02:45	167	5.0	0.97	443.4	13.0 ± 1.8	24.9 ± 1.1	78.2 ± 2.3	78.6 ± 22.3
	3	622.1	03:16	124	2.3	0.88	326.0	12.0 ± 2.1	22.3 ± 0.9	66.0 ± 1.5	47.3 ± 8.2
	4	634.4	03:18	132	4.2	1.01	308.7	13.0 ± 1.0	32.1 ± 1.5	50.8 ± 1.6	46.9 ± 7.2
	3	529.6	03:53	155	3.4	1.02	122.1	28.0 ± 4.7	39.0 ± 2.8	64.9 ± 1.8	32.3 ± 12.5
PartB	4	446.9	04:39	166	4.7	1.17	102.5	29.0 ± 6.1	46.2 ± 4.6	43.5 ± 0.7	20.3 ± 8.4
	3	637.6	03:12	146	4.8	1.08	217.0	26.0 ± 3.5	46.3 ± 2.1	55.2 ± 0.9	54.3 ± 18.7
PartC	4	474.2	04:24	128	3.3	1.04	147.7	25.0 ± 2.4	63.3 ± 2.6	33.8 ± 1.8	28.2 ± 9.2

bpm, beats per minute; min, minutes; spm, strokes per minute; cm, centimeters.

Drive phase duration indicates the timing of when the participant transitioned from the drive phase to the recovery phase.

Table 9- Performance and physiological variables presented as single values or mean ± SD for the participants in the four different setups.

Chapter 4 - Results and Discussion

Table 9 presents the results of post-hoc comparisons for various biomechanical parameters, along with descriptive information related to performance and physiological variables. The variables Distance [m], Mean Power Output [W], and Time/500 m [min] are obtained from the RP3 Rowing Lite application and offer a broad perspective on rowing performance. Physiological data is represented by variables such as Heart Rate (HR) [bpm], Blood Lactate (BLa) [mmol/L], and Respiratory Exchange Ratio (RER), providing insights into the athlete's overall fatigue state. Additional parameters include Peak Handle Force [N], Drive Phase Duration [%], Stroke Rate [spm], Stroke Length [cm], and P_{rower} [W] collectively contribute to a comprehensive understanding of the system's biomechanics.

The RER value and BLa levels across all participants in different conditions demonstrate a submaximal intensity state with no observable signs of fatigue, aligning with the intended outcome. Notably, the RER value closely approximates 1. Furthermore, it is evident that the introduction of additional constraints generally leads to a reduction in HR. The distance covered during the 4-minute rowing sessions decrease across different setups for all participants, as does the mean power output. It's interesting to note that the technique employed throughout the setups, as evidenced by the variable Drive Phase duration, typically maintains a consistent pattern.

4.1 Stroke length, stroke rate, and total power

In Figure 19 are presented the average *stroke length* LS , *stroke rate* SR , and total power P_{rower} of each participant during the four different setups.

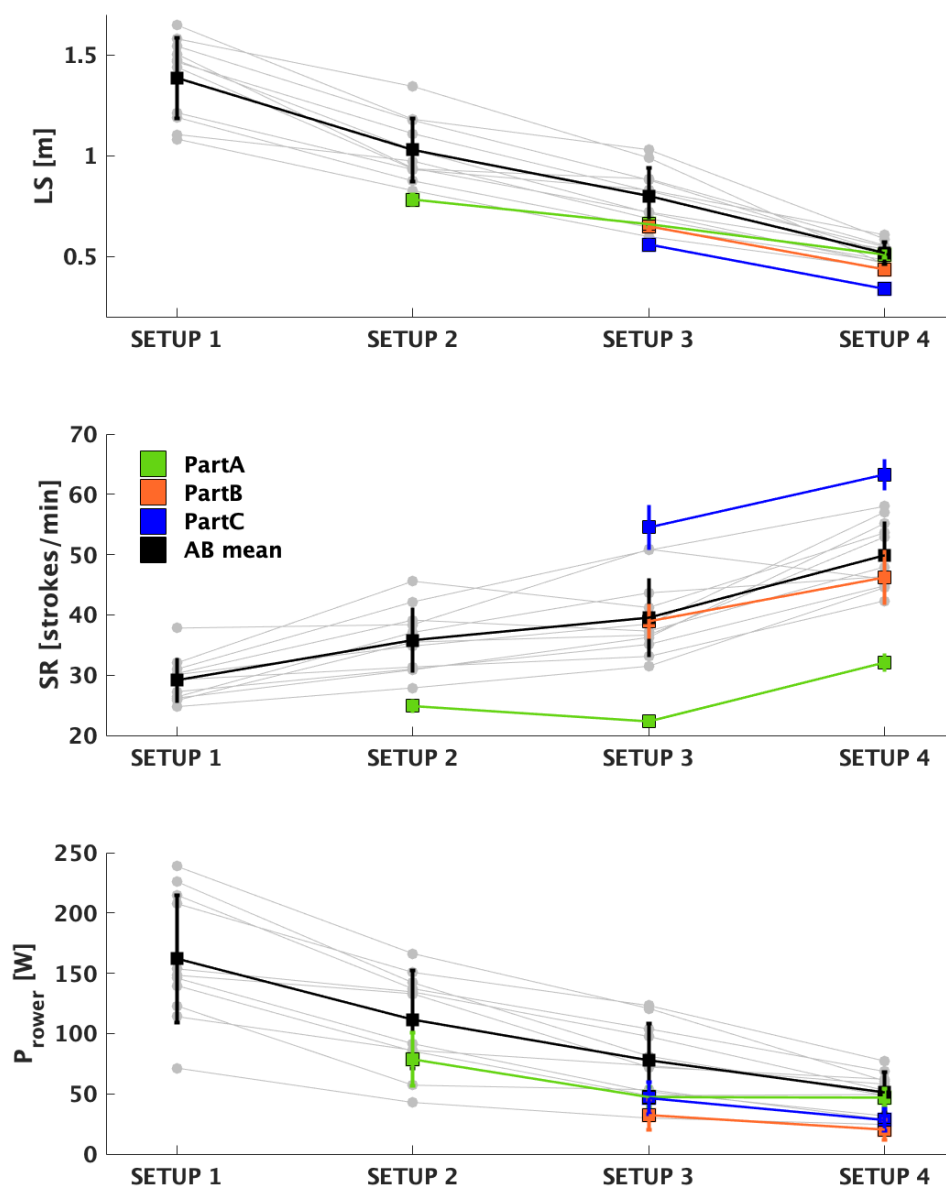


Figure 19 - Stroke Length LS , Stroke Rate SR , Power generated by the rower. AB participants are reported in grey, while mean \pm SD of the AB group is reported in black. Participants with physical impairments are reported separately as PartA, PartB, and PartC with the colors in the legend.

Chapter 4 - Results and Discussion

For the AB group, typically there is a noticeable behavior in the data. The stroke length (LS) consistently decreases in a linear behavior as additional movement constraints are introduced, starting from setup 2 where the seat is fixed, and further limiting trunk movement in setup 3. Simultaneously, the stroke rate (SR) exhibits a linear increase and, P_{rower} (power generated by the rower) follows the pattern of LS, decreasing progressively across the setups.

Participant A, in the SR graph from setup 2 to setup 3, does not follow the AB group behavior. Throughout all setups, participant A consistently maintains a lower SR compared to the other participants, despite similar trends in the LS and power (P_{rower}) graphs. This observation may suggest a distinct rowing technique, as indicated by the Driving Phase variable: Setup 2 - PartA $13.0 \pm 1.8\%$, AB $23.1 \pm 2.4\%$; Setup 3 - PartA $12.0 \pm 2.1\%$, AB $21.8 \pm 3.3\%$; Setup 4 - PartA $13.0 \pm 1.0\%$, AB $20.8 \pm 2.8\%$ (Table 9). However, it should be noted that the abnormal behavior is due to setup 3. Specifically, Table 9 highlights that the distance covered during Setup 3 is shorter than that in Setup 4 (Setup 3: 622.1 m, Setup 4: 634.4 m). Furthermore, the BL_a value in Setup 3 is notably lower than in the other configurations (Setup 2: 5 mmol/L, Setup 3: 2.3 mmol/L, Setup 4: 4.2 mmol/L), as the heart rate (Setup 2: 167 bpm, Setup 3: 124 bpm, Setup 4: 132 bpm). These findings suggest that the prescribed intensity for participant A in setup 3 was potentially miscalculated (RER Setup 3: 0.88).

Participant C, in the SR graph shows higher values than all the participants (Setup 3 - PartC 46.3 ± 2.1 spm, AB 39.5 ± 2.5 spm; Setup 4 - PartC 63.3 ± 2.6 spm, AB 49.9 ± 2.3 spm) with a low LS (Setup 3 - PartC 55.2 ± 0.9 cm, AB 80.0 ± 2.1 cm; Setup 4 - PartC 38.8 ± 1.8 cm, AB 51.6 ± 1.3 spm) despite having comparable power to the other participants.

4.2 Force handle

The unidirectional force applied to the handle is shown in the Figure 20. This graph is useful to highlight different techniques.

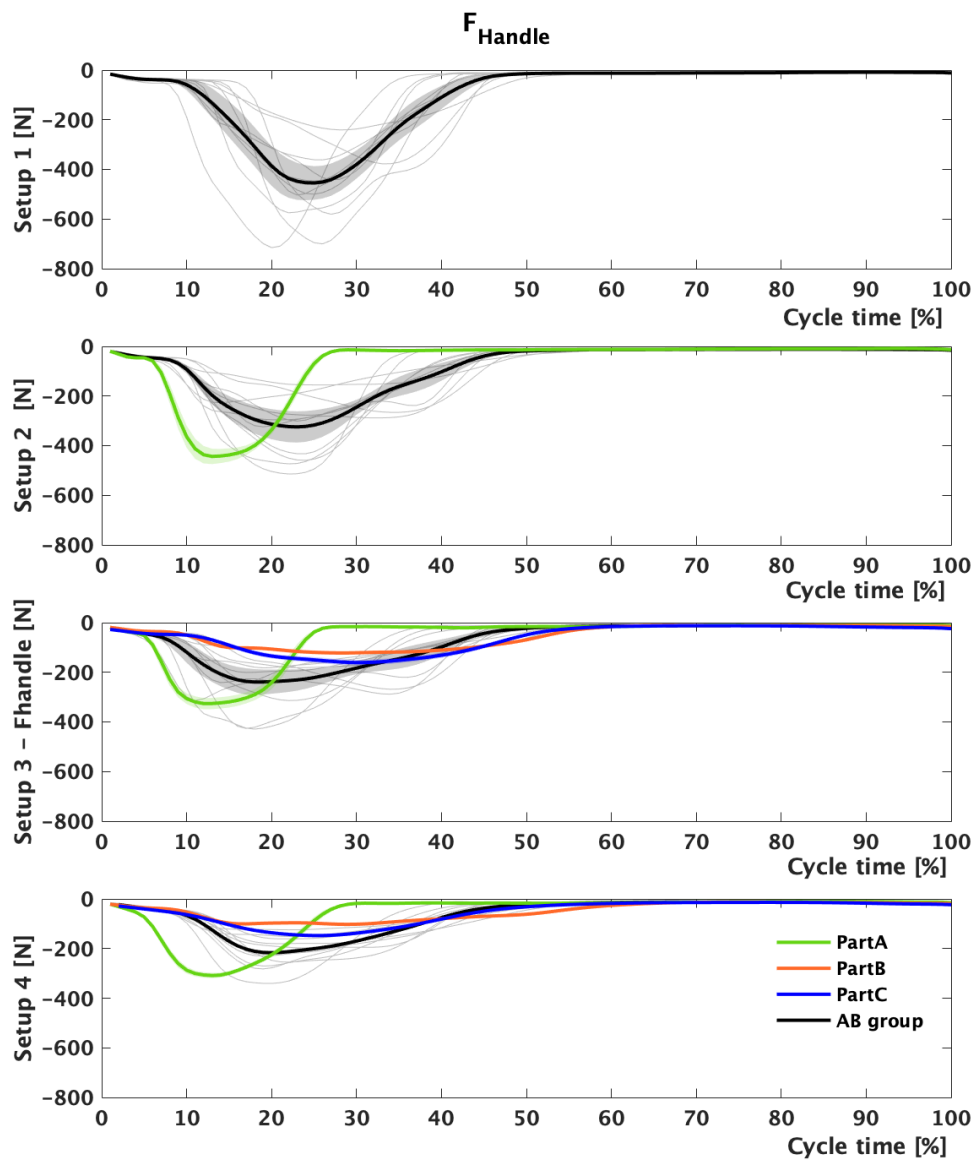


Figure 20 - Force handle among the four setups. AB participants are reported in gray, AB mean \pm SD is reported in black and participants with physical disabilities are reported with different colors as in the legend.

It is visible that also for the AB group there is not homogeneity in the technique of rowing. This can be caused by the fact that participants are not professional rowers.

Chapter 4 - Results and Discussion

Participant A shows a different technique than the AB group in all the setups. To gain a more in-depth understanding of these variations, we can report the force F_{handle} measured during the rowing cycle as reported in Figure 20. Participant A consistently demonstrates a notably shorter driving phase compared to the rest of the AB participants across all setups. In setups 3 and 4, Participant A's technique also features a higher peak force when compared to the majority of the AB participants. Remarkably, despite these

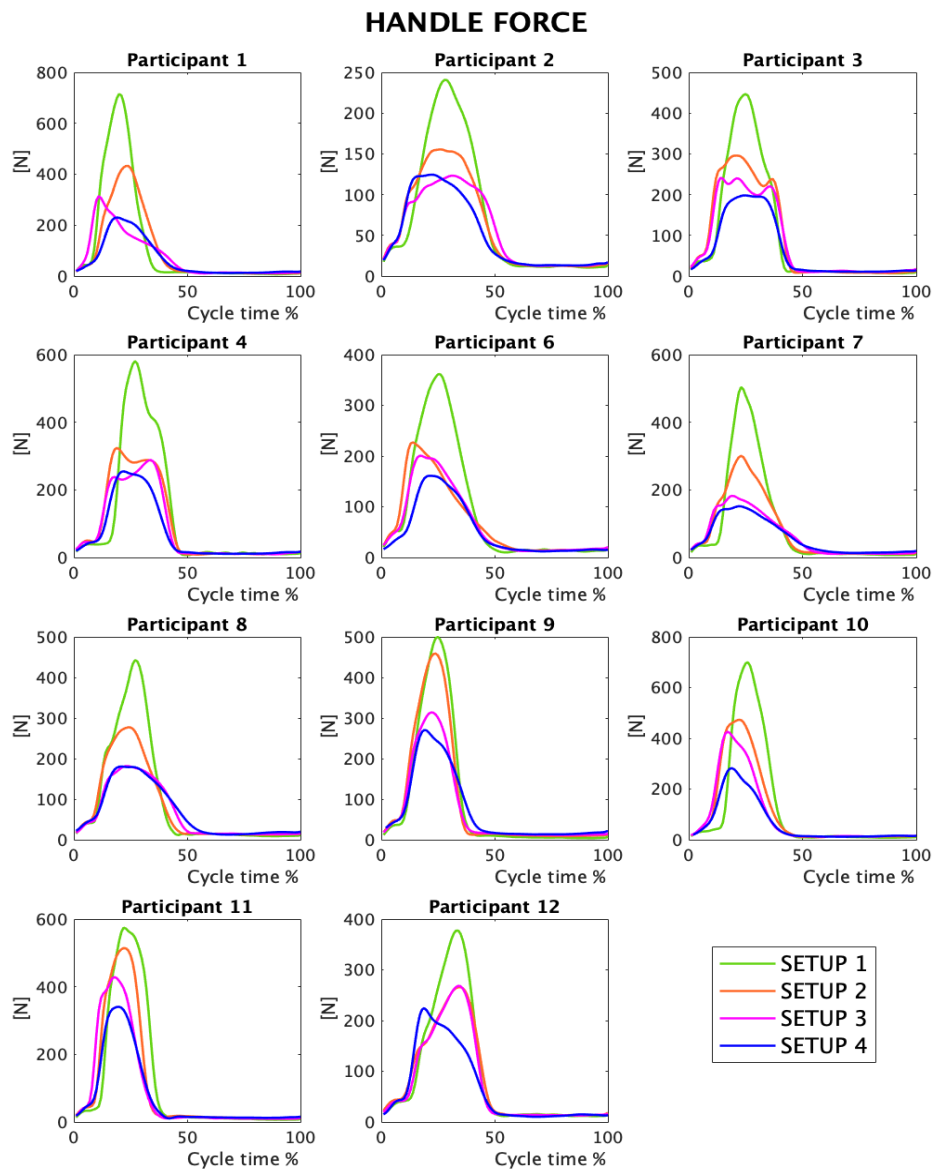


Figure 21 – The grid graph displays the handle force for all participants within the AB group. This visualization is valuable for discerning variations in rowing techniques among the participants.

Chapter 4 - Results and Discussion

differences, Participant A maintains a consistent rowing technique throughout the different setups, displaying a remarkable degree of stability in his approach.

A more detailed analysis of the AB group, as illustrated in Figure 21, reveals further insights. Particularly, participants like Participant 1 and Participant 3 undergo substantial changes in their rowing technique when exposed to the various motor constraints introduced by different setups. On the other hand, participants such as Participant 6, 10, and 11 maintain relatively consistent handle force patterns. However, a noticeable shift to the left in peak force becomes apparent as the setups progress. This shift is associated with a shorter duration of the driving phase, indicating a potential adjustment to the new constraints introduced by these setups.

These findings suggest that participants with physical disabilities may possess a greater capacity for adapting to changes in motor constraints, leading to diverse techniques within the AB group.

4.3 Total power generated by the rower

An in-depth examination of P_{rower} (total power generated by the rower) behavior throughout the rowing cycle is necessary.

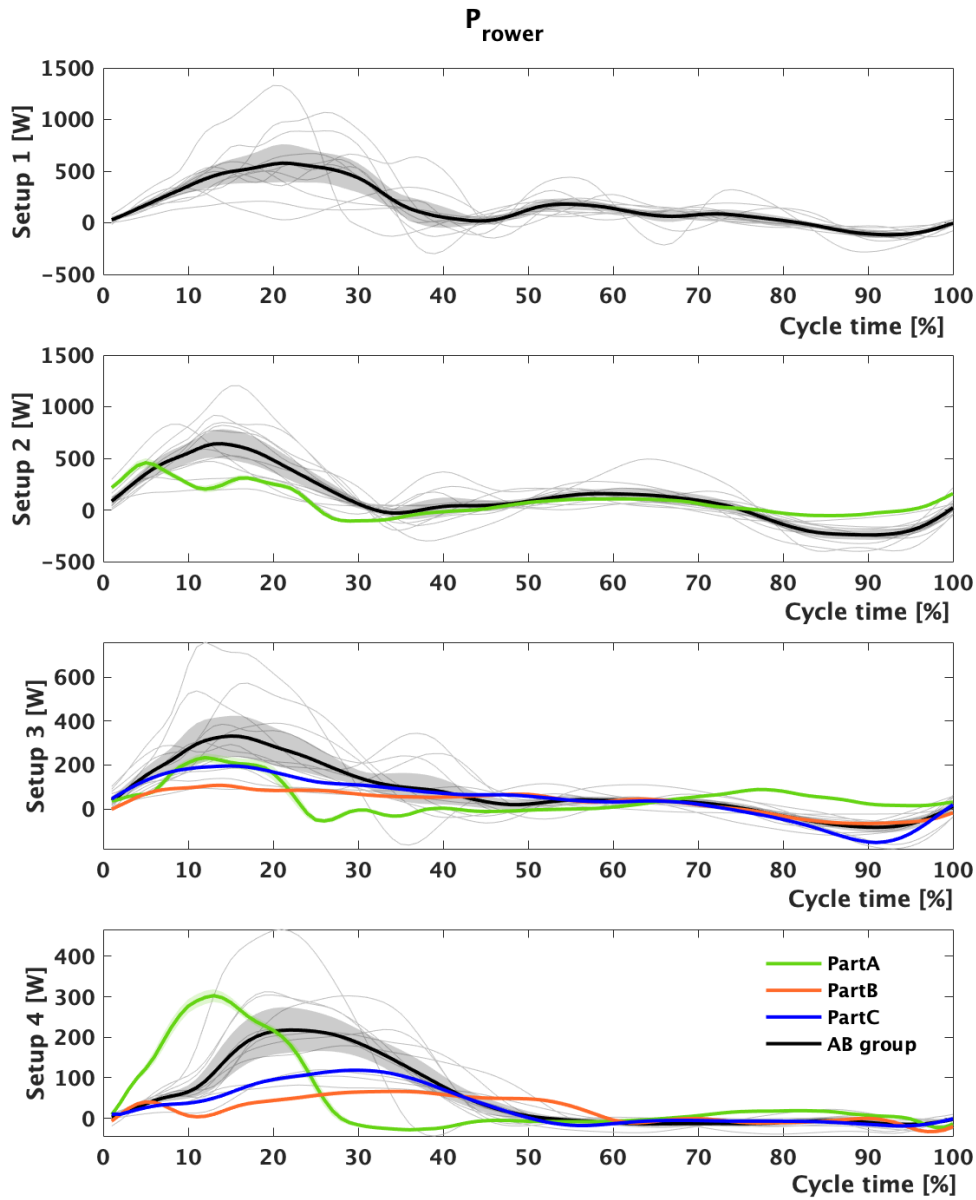


Figure 22 - Power generated by the rower, calculated as outlined in Section 3.4.9.

Specifically, as observed in Figure 22, the behavior of participants within the AB group exhibits notable variations that are neither uniform nor consistent across the different setups.

Chapter 4 - Results and Discussion

Participant B and Participant C consistently display similar behaviors in setups 3 and 4. In contrast, Participant A, as seen in the handle force analysis, exhibits distinct patterns from the AB group. Notably, in setup 2 and 3, his behavior closely aligns with that of the AB group, but in setup 4, he demonstrates a notably higher peak power compared to the mean peak of the AB group. Furthermore, the peak power in setup 4 (302 W) significantly surpasses the peak power in setups 3 (233 W), while the mean P_{rower} values in these two setups are similar (Setup 3: 47.3 ± 8.2 W; Setup 4: 46.9 ± 7.2 W). This behaviour points to two plausible explanations: firstly, the notion that, for Participant A, the capacity to generate power using the trunk may not yield a discernible impact compared to scenarios where such utilization is restricted. Alternatively, it raises the prospect that an error might have occurred in determining the appropriate intensity for setup 3, as previously hypothesized in Section 4.1. A comprehensive understanding of this behavior necessitates an examination of the Range of Motion (ROM) analysis and a deeper dive into the analysis of power generated by individual joints.

4.4 Range of motion

The subsequent paragraphs delve into the range of motion (ROM) of each segment. The nomenclature and convention used to express the segment angle ROM aligns with the explanation provided in section 3.4.8. For quick reference, Table 6 is reiterated here.

ANGLE NAME CONVENTION		
Expressed segment	in LCS of	Angle name
Forearm	Arm	Elbow
Arm	Trunk/Up-trunk	Shoulder
Trunk / Up-trunk	ICS	Trunk
Pelvis	ICS	Pelvis
Thigh	ICS	Thigh
Shank	Thigh	Knee
Foot	Shank	Ankle

Table 6 - Nomenclature convention employed to denote the angles of the body segments based on the Local Coordinate System (LCS) used for their expression.

It's crucial to remember that the definition of the trunk angle varies depending on the setup. In setups 1 and 2, it represents the angle between the trunk segment and the ICS. Conversely, in setups 3 and 4, it denotes the angle between the up-trunk segment and the ICS. Additionally, in setups 3 and 4, due to the fact that they are fixed, the pelvis, thigh, knee, and ankle joints are not considered. Moreover, PartB, and PartC did not perform in setups 1 and 2, and therefore, their data is omitted in the pelvis, ankle, knee, and thigh angles.

For a comprehensive analysis, figures from Figure 23 to Figure 29 offer detailed insights into the ROM of each segment. These figures highlight disparities between the AB group, presented both individually and as mean \pm SD, and the Participants with physical impairments.

4.4.1 Elbow

Figure 23 focuses on the ROM of elbow angles as flexion/extension and pronation/supination.

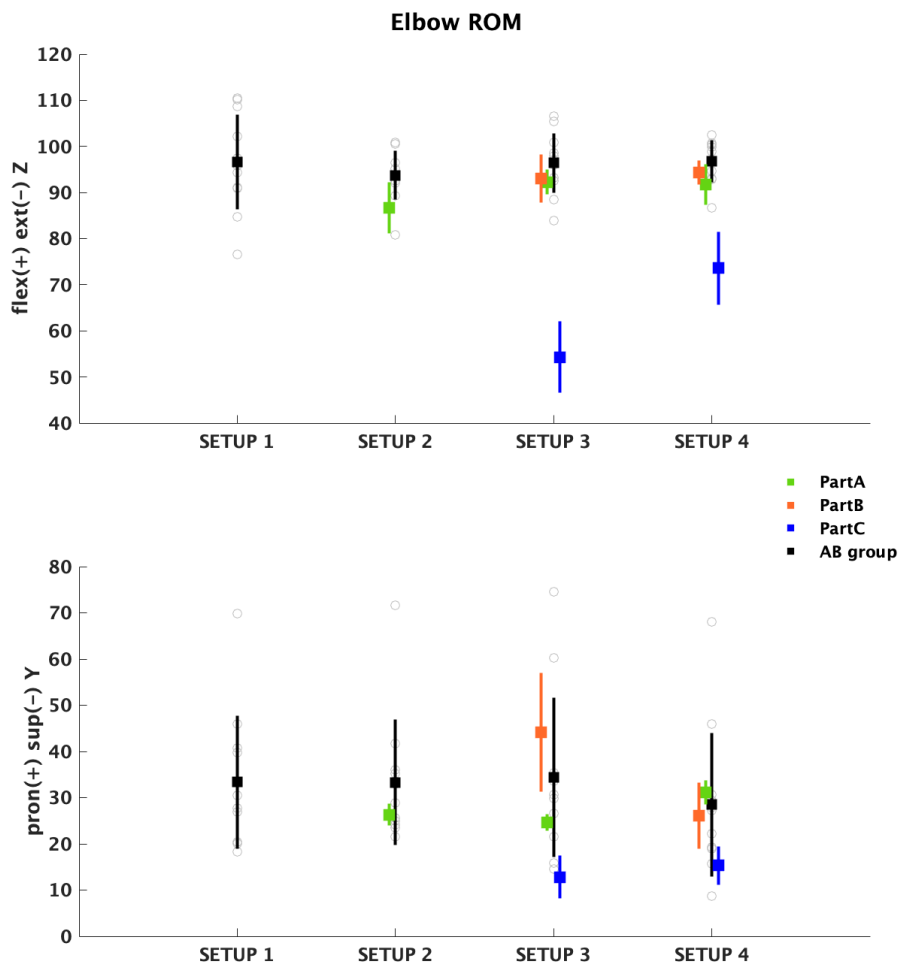


Figure 23 -ELBOW ROM [deg]: Flexion/Extension, Pronation/Supination. AB participants are reported in grey, while mean \pm SD of the AB group is reported in black. Values for participants with physical impairments are presented as mean \pm SD, with colors corresponding to the legend.

It is interesting to note that elbow angles for the AB group are not affected by the motion restriction introduced along the setups (Flexion/Extension Setup 1: 96.5 ± 10.4 deg; Setup 2: 93.7 ± 5.3 deg; Setup 3: 96.4 ± 6.4 deg; Setup 4: 96.8 ± 4.6 deg), (Pronation/Supination Setup 1 – 33.3 ± 14.4 deg; Setup 2 – 33.4 ± 13.5 ; Setup 3 – 34.3 ± 17.2 ; Setup 4 – 28.5 ± 15.5).

		ELBOW ROM [deg]	
		Flexion Extension	Pronation Supination
AB group	1	96.5 ± 10.4	33.3 ± 14.4
	2	93.7 ± 5.3	33.3 ± 13.5
	3	96.4 ± 6.4	34.3 ± 17.2
	4	96.8 ± 4.6	28.5 ± 15.5
PartA setup	2	86.7 ± 5.5	26.3 ± 2.4
	3	92.3 ± 2.7	24.6 ± 1.8
	4	91.7 ± 4.4	31.1 ± 2.6
PartB	3	93.0 ± 5.2	44.2 ± 12.9
	4	94.4 ± 2.6	26.1 ± 7.2
PartC	3	54.3 ± 7.8	12.8 ± 4.6
	4	73.6 ± 7.9	15.3 ± 4.1

Table 10 - Range of Motion (ROM) of the elbow, expressed in degree. Values are reported as mean ± SD. The elbow angle is considered between the forearm segment and the arm segment.

Participant C, both in setup 3 and setup 4, demonstrates a reduced ROM, for the flexion/extension, compared to the AB group. Particularly in setup 3, the difference is around 40 degrees (Setup 3: PartC 54.3±7.8 deg; Setup 4: PartC 73.6±7.9 deg). To comprehend the varying behavior of PartC from Setup 3 to Setup 4, it is essential to refer back to Table 9 and Figure 19, which revealed a shorter stroke length (Setup 3 – PartC 55.2±0.9cm, AB 80.0±2.1cm; Setup 4 – PartC 38.8±1.8cm, AB 51.6±1.3spm) and higher stroke rate (Setup 3 – PartC 46.3±2.1spm, AB 39.5±2.5spm; Setup 4 – PartC 63.3±2.6spm, AB 49.9±2.3spm) for PartC compared to the AB group. It is worth noting that, per the protocol, participants began measurements with setup 4 and then proceeded to setup 3. This sequence may have induced increased elbow fatigue in PartC, limiting her ability to achieve a greater ROM in setup 3. This hypothesis finds support in various studies reporting that fatigue is a common symptom in individuals with spinocerebellar ataxia [57-60].

Chapter 4 - Results and Discussion

Regarding the pronation/supination angle ROM, in setup 3, Participant B displays a slightly higher ROM than the AB group, although it still falls within the range of the AB group's standard deviation (Setup 3 – PartB 44.2 ± 12.9 deg). Conversely, in setup 3, Participant C shows a smaller ROM value than the AB group (Setup 3 – PartC 12.8 ± 4.6 deg). This observation may be connected to what was previously assessed for flexion/extension ROM.

4.4.2 Shoulder and Trunk

Figure 24 centers on the ROM of shoulder angles as flexion/extension, adduction/abduction, and internal/external rotation. Additionally, Figure 25 focuses on the ROM of trunk angles as flexion/extension, adduction/abduction, and internal/external rotation.

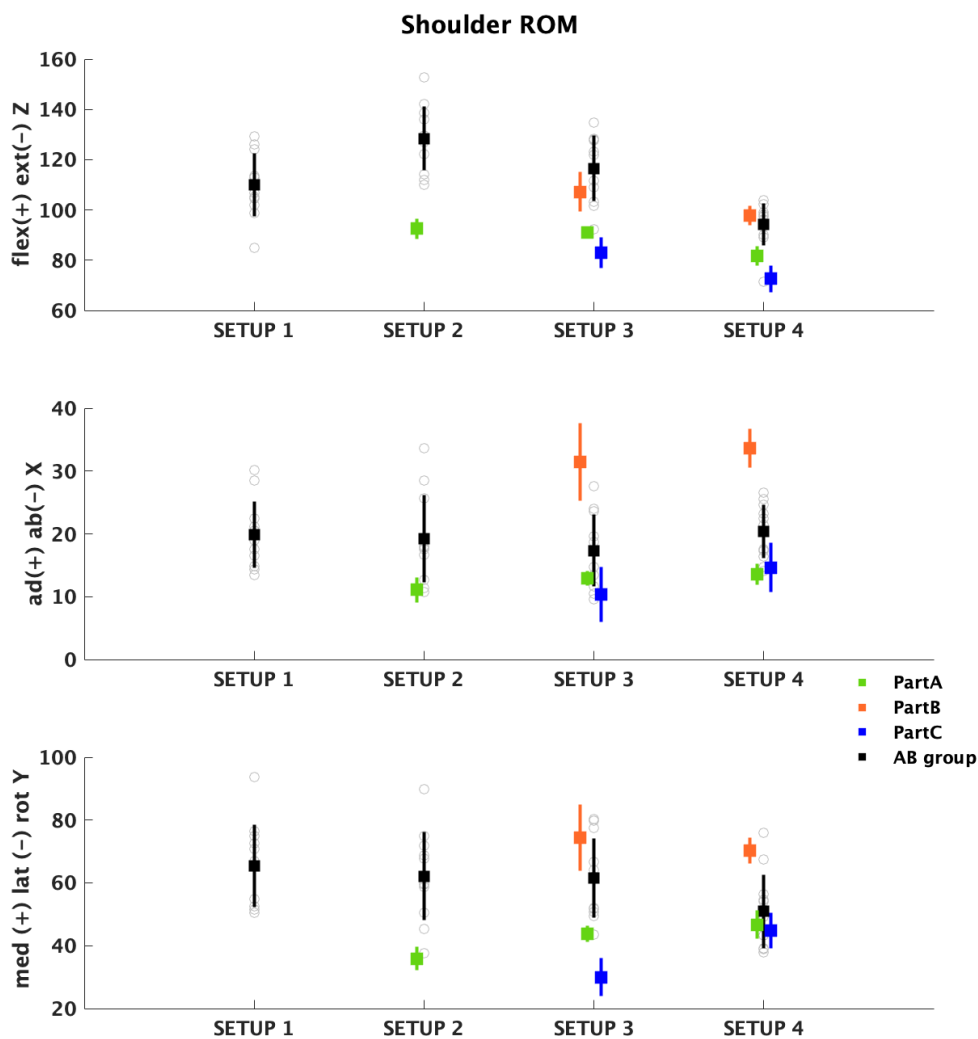


Figure 24 - SHOULDER ROM [deg]: Flexion/Extension, Adduction/Abduction, Medial/Lateral rotation. AB participants are reported in grey, while mean \pm SD of the AB group is reported in black. Values for participants with physical impairments are presented as mean \pm SD, with colors corresponding to the legend.

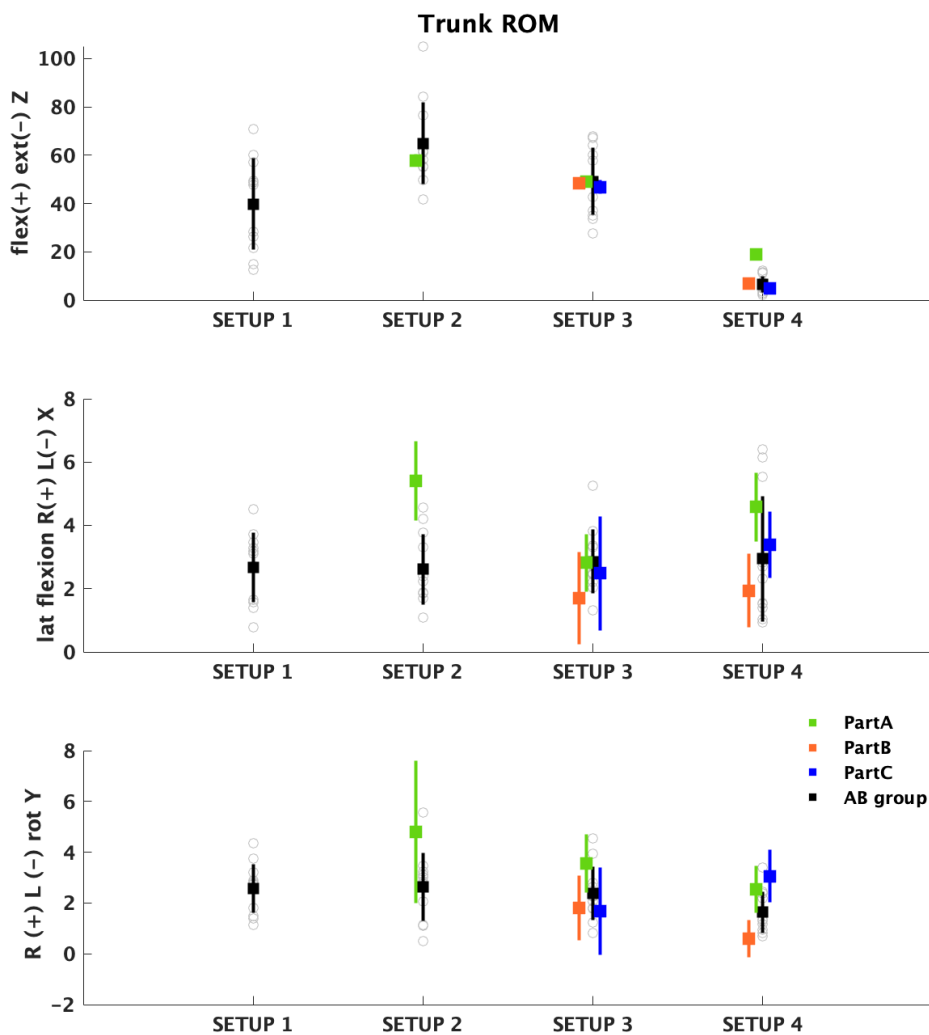


Figure 25 - TRUNK ROM [deg]: Flexion/Extension, lateral trunk flexion Right/Left, Right/Left Rotation. AB participants are reported in grey, while mean \pm SD of the AB group is reported in black. Values for participants with physical impairments are presented as mean \pm SD, with colors corresponding to the legend.

Chapter 4 - Results and Discussion

		SHOULDER ROM [deg]		
		Flexion Extension	Adduction Abduction	Medial Lateral rotation
AB group	1	109.9 ± 12.6	19.9 ± 5.2	65.4 ± 13.2
	2	128.4 ± 12.7	19.2 ± 6.9	62.2 ± 13.9
	3	116.5 ± 13.0	17.3 ± 5.7	61.6 ± 12.6
	4	94.2 ± 8.4	20.4 ± 4.3	50.9 ± 11.8
PartA setup	2	92.5 ± 4.0	11.1 ± 1.9	35.9 ± 3.8
	3	90.9 ± 2.3	13.0 ± 1.2	43.9 ± 2.6
	4	81.8 ± 3.8	13.6 ± 1.7	46.7 ± 4.4
PartB	3	107.2 ± 7.8	31.4 ± 6.2	74.5 ± 10.6
	4	97.7 ± 3.8	33.6 ± 3.1	70.3 ± 4.2
PartC	3	82.9 ± 6.2	10.4 ± 4.4	30.0 ± 6.1
	4	72.5 ± 5.4	14.7 ± 4.0	44.7 ± 5.7

Table 11 - Range of Motion (ROM)of the shoulder, expressed in degree. Values are reported as mean ± SD. The shoulder angle is considered between the arm segment and the trunk/up-trunk segment.

		TRUNK ROM [deg]		
		Flexion Extension	Lateral trunk flexion Right Left	Right Left rotation
AB group	1	39.7 ± 18.9	2.7 ± 1.1	2.6 ± 1.0
	2	64.9 ± 16.9	2.6 ± 1.1	2.6 ± 1.3
	3	49.2 ± 14.0	2.9 ± 1.0	2.4 ± 1.0
	4	6.7 ± 3.4	2.9 ± 2.0	1.6 ± 0.8
PartA setup	2	57.8 ± 2.5	5.4 ± 1.3	4.8 ± 2.8
	3	49.0 ± 1.8	2.8 ± 0.9	3.6 ± 1.1
	4	19.0 ± 1.5	4.6 ± 1.1	2.5 ± 0.9
PartB	3	48.4 ± 1.8	1.7 ± 1.5	1.8 ± 1.3
	4	6.9 ± 1.1	1.9 ± 1.2	0.6 ± 0.7
PartC	3	46.8 ± 2.9	2.5 ± 1.8	1.7 ± 1.7
	4	4.8 ± 2.2	3.4 ± 1.1	3.1 ± 1.0

Table 12 - Range of Motion (ROM)of the trunk, expressed in degree. Values are reported as mean ± SD. The trunk angle is considered between the trunk/up-trunk segment and the ICS.

Chapter 4 - Results and Discussion

The analysis of the shoulder flexion/extension angle ROM is closely linked to the analysis of the trunk one. In fact, restricting trunk movement limits shoulder movement, preventing the achievement of high angles in both flexion and extension. Specifically, as visible in the AB group, moving from setup 1 to setup 2, the constraint on the sliding seat results in greater trunk flexion and extension (Setup 1 - 39.7 ± 18.9 deg; Setup 2 - 64.9 ± 16.9 deg) allowing for a higher ROM of the shoulder flexion/extension from 109.9 ± 12.6 deg to 128.4 ± 12.7 deg. Conversely, transitioning from Setup 3 to Setup 4, the introduction of a backrest considerably restricts trunk flexion/extension (Setup 3 - 49.2 ± 14.0 deg; Setup 4 - 19.0 ± 1.5 deg), consequently reducing the shoulder ROM (Setup 3 - 116.5 ± 13.0 deg; Setup 4 - 94.2 ± 8.4 deg).

Participant A follows a similar behavior to the AB group across setups but exhibits a smaller ROM of the shoulder flexion/extension angle compared to the AB group (Setup 2 - 92.5 ± 4.0 deg; Setup 3 - 90.0 ± 2.3 deg; Setup 4 - 81.8 ± 3.8 deg).

Participant C mirrors the AB group's behavior from setup 3 to setup 4 in both shoulder and trunk flexion/extension, however the ROM value for the shoulder is smaller than the AB group (Setup 3 - 82.9 ± 6.2 deg; Setup 4 - 72.6 ± 5.4 deg).

The AB group exhibits consistent behavior across the setups for angles in the other planes, such as adduction/abduction (X-axis) and medial/lateral rotation (Y-axis) for the shoulder, and lateral trunk flexion (X-axis) and right/left rotation (Y-axis) for the trunk.

Participant B, although she follows the AB group in the flexion/extension, exhibits different behavior in both the other rotation planes of the shoulder. In particular, in the adduction/abduction angle of the shoulder, she demonstrates a higher ROM (Setup 3 - PartB 31.4 ± 6.2 deg, AB group 17.3 ± 5.7 deg; Setup 4 - PartB 33.6 ± 3.1 deg, AB group 20.4 ± 4.3 deg). In the medial/lateral rotation ROM of the shoulder, she also exhibits higher values than the AB group (Setup 3 - PartB 74.5 ± 10.6 deg, AB group 61.6 ± 12.6 deg; Setup 4 - PartB 70.3 ± 4.2 deg, AB group 50.9 ± 11.8 deg) although the difference is less pronounced, and in setup 3, her ROM aligns with the AB

Chapter 4 - Results and Discussion

group variation. This behavior may be attributed to her impairment. In fact, studies in the literature report that the shoulder is a joint subject to severe instability in individuals with Ehlers-Danlos syndrome [61-63].

Participant C not only exhibits a difference in shoulder flexion/extension but also demonstrates a smaller ROM in the shoulder's medial/lateral rotation angle compared to the AB group, especially in setup 3 (PartC 30.0 ± 6.1 deg). However, in setup 4, she aligns with the behavior of the AB group. This discrepancy in the ROM of the shoulder's medial/lateral angle may be influenced by similar factors observed in the elbow movement.

4.4.3 Pelvis

The pelvis ROM angles are reported only for setup 1 and 2 because in setup 3 and 4, we assume them as stationary and do not analyze them. Consequently, there is only one participant with physical impairments that did setup 2, and it is PartA.

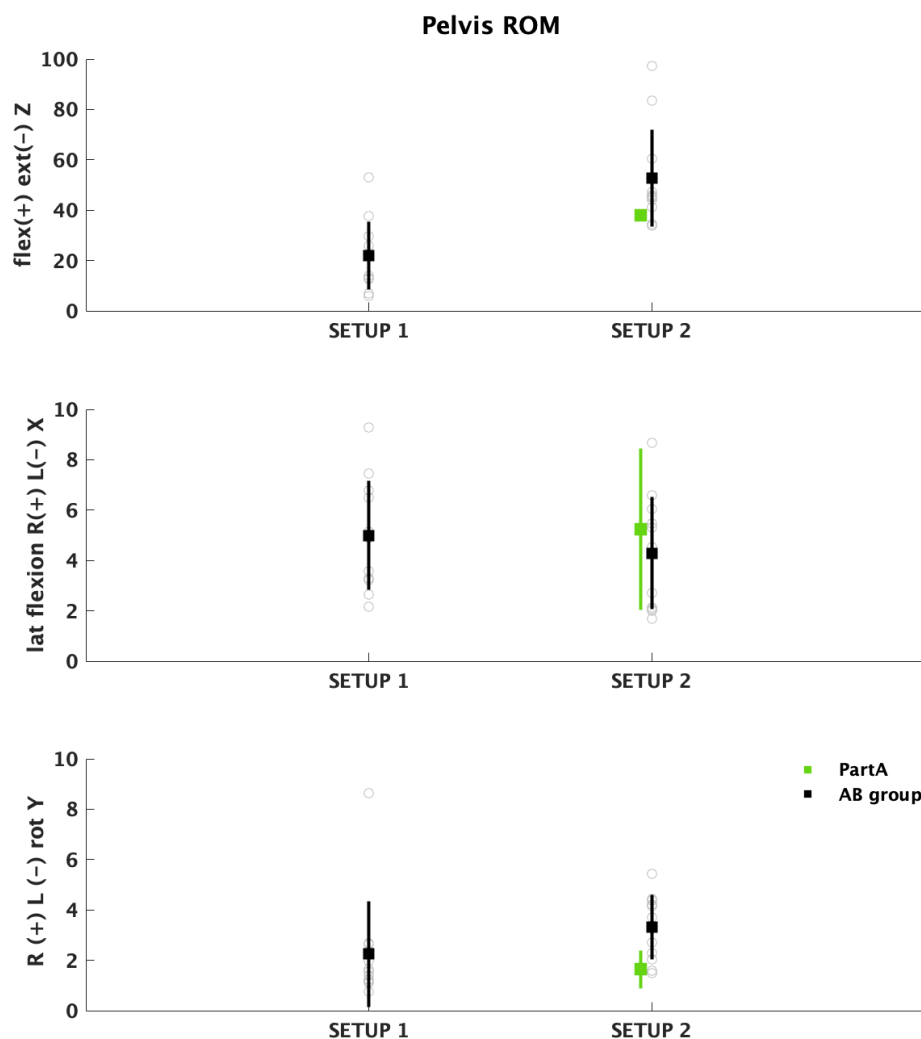


Figure 26- PELVIS ROM [deg]: Flexion/Extension, Lateral pelvis flexion Right/Left, Right/Left Rotation. AB participants are reported in grey, while mean \pm SD of the AB group is reported in black. Values for participants with physical impairments are presented as mean \pm SD, with colors corresponding to the legend. The pelvis angle is analyzed only in setup 1 and 2, and consequently, PartB and PartC are not included in the analysis

Chapter 4 - Results and Discussion

		PELVIS ROM [deg]		
		Flexion Extension	Lateral pelvis flexion Right Left	Right Left rotation
PartA AB group	1	22.1 ± 7.3	5.0 ± 2.1	2.2 ± 1.1
	2	52.6 ± 19.5	4.3 ± 1.9	3.3 ± 1.3
	2	38.1 ± 2.2	5.2 ± 3.2	1.6 ± 0.8

Table 13 - Range of Motion (ROM) of the pelvis, expressed in degree. Values are reported as mean ± SD. The pelvis angle is considered between the pelvis segment and the ICS.

From Figure 26, it is visible that going from setup 1 to setup 2, adding a constraint on the leg, increased the flexion/extension ROM for the AB group (Setup 1 - 22.1±7.3 deg; Setup 2 - 52.6±19.5 deg). The angles in the other planes, such as lateral pelvis flexion and right/left rotation, exhibit a consistent behavior across the setups with small values, indicating minimal movement in those planes.

The comparison of the pelvis angle behavior for Participant A is possible only in setup 2, so it is not possible to evaluate his changes across the setups. However, we can still compare his behavior in setup 2 to the AB group. In this case, he shows a similar behavior to the AB group in all the planes (PartA: Setup 2 – flex/ext 38.1±2.2 deg; lateral flexion 5.2±3.2 deg; R/L rot 1.6±0.8 deg).

4.4.4 Thigh

The thigh angles are reported only for setup 1 and setup 2, and are expressed between the thigh segment and the ICS.

In setup 2, where leg movement is restricted, we expect to observe a small ROM for the thigh.

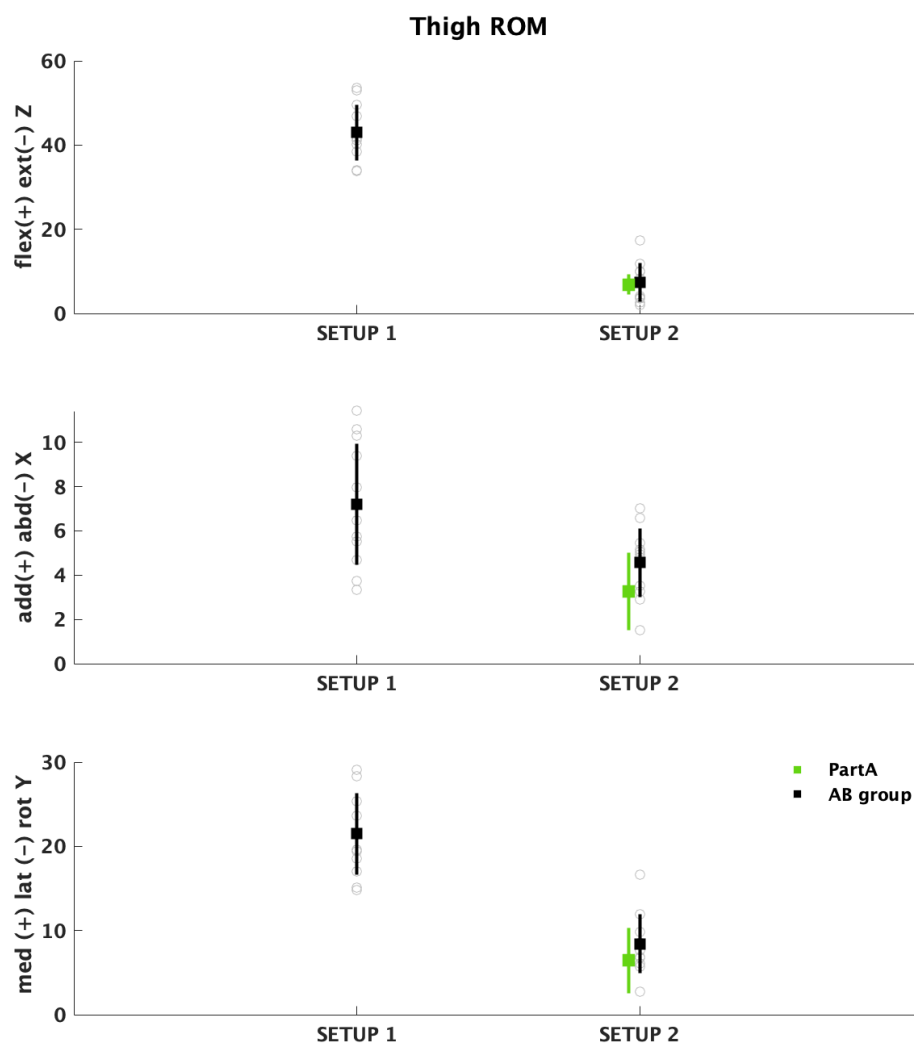


Figure 27 - THIGH ROM [deg]: Flexion/Extension, Adduction/Abduction, Medial/Lateral rotation. AB participants are reported in grey, while mean \pm SD of the AB group is reported in black. Values for participants with physical impairments are presented as mean \pm SD, with colors corresponding to the legend. The thigh angle is analyzed only in setup 1 and 2, and consequently, PartB and PartC are not included in the analysis.

Chapter 4 - Results and Discussion

		THIGH ROM [deg]		
		Flexion Extension	Adduction Abduction	Medial Lateral rotation
PartA AB group	1	42.9 ± 6.6	7.2 ± 2.7	21.5 ± 4.9
	2	7.4 ± 4.5	4.6 ± 1.6	8.4 ± 3.5
	2	6.9 ± 2.4	3.3 ± 1.7	6.5 ± 3.9

Table 14 - Range of Motion (ROM) of the thigh, expressed in degree. Values are reported as mean ± SD. The thigh angle is considered between the thigh segment and the ICS.

Figure 27 illustrates the thigh angles ROM, highlighting that for the AB group, the flexion/extension ROM decreases significantly, as expected (Setup 1 - 42.9±6.6 deg; Setup 2 - 7.4±4.5 deg). The adduction/abduction angle, despite having a relatively small ROM even in setup 1 (Setup 1 - 7.2±2.7 deg), slightly decreases but remains different from zero (Setup 2 - 4.6±1.6 deg). The medial/lateral rotation angles exhibit a similar trend to the flexion/extension one, indeed from setup 1 to setup 2 the ROM decrease from 21.5± 4.9. deg to 8.4±3.5 deg.

Participant A, displayed a behavior in setup 2 similar to the AB group. Despite the restricted leg movement, there was a small yet noticeable movement in the thigh (flex/ext 6.9±2.4 deg; add/abd 3.3±1.7 deg; med/lat rot 6.5±3.9 deg). Further exploration in the power analysis, particularly comparing the power produced in his hip to that produced by the AB group, will be interesting.

4.4.5 Knee and Ankle

We report the knee and ankle angle ROM analysis together because being reported only for setup 1 and 2 we expect a similar behavior. Particularly we expect to see a severe decrease in the movement.

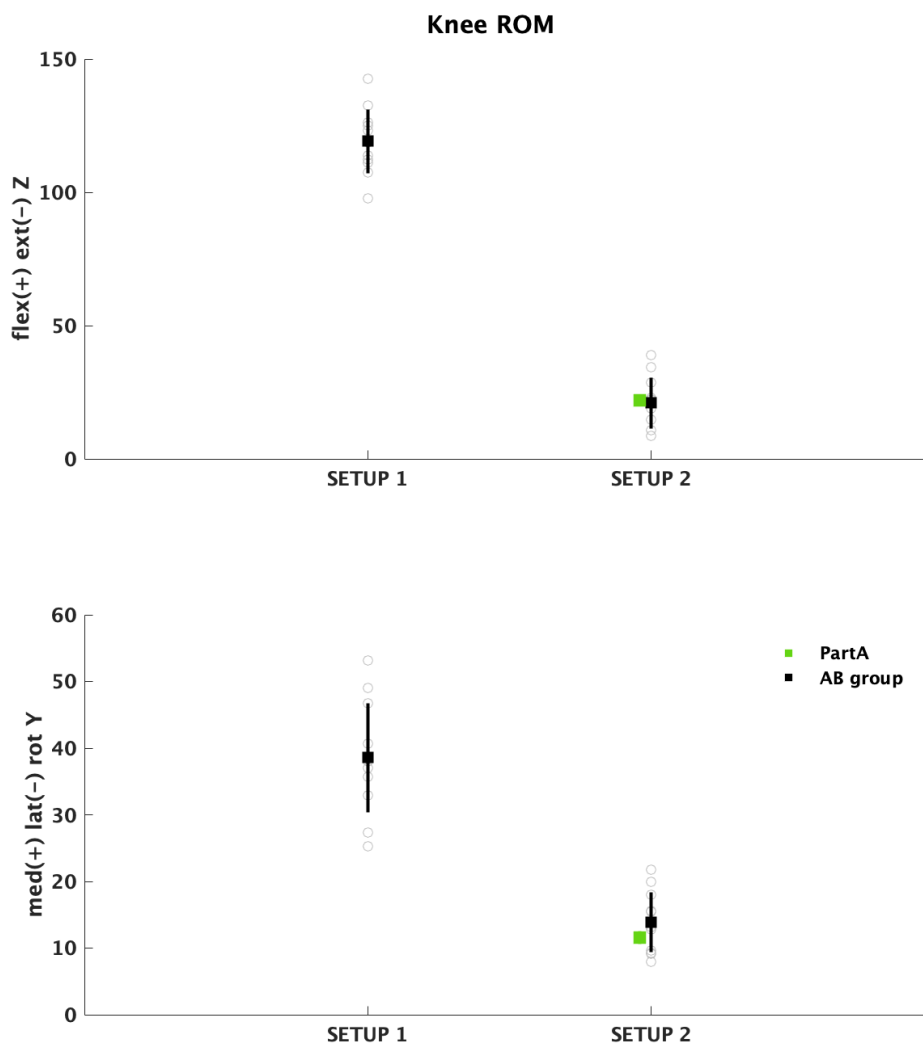


Figure 28 - KNEE ROM [deg]: Flexion/Extension, Medial/Lateral rotation. AB participants are reported in grey, while mean \pm SD of the AB group is reported in black. Values for participants with physical impairments are presented as mean \pm SD, with colors corresponding to the legend. The knee angle is analyzed only in setup 1 and 2, and consequently, PartB and PartC are not included in the analysis.

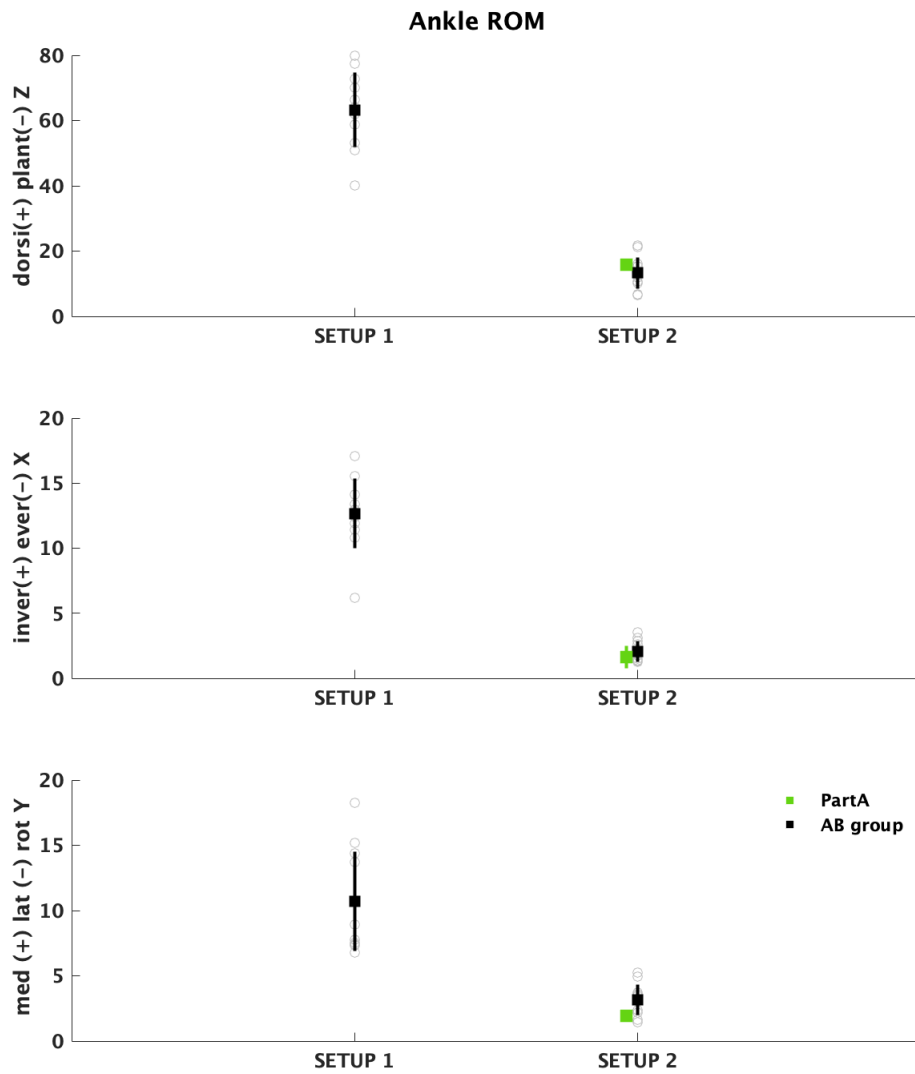


Figure 29 - ANKLE ROM [deg]: dorsiflexion/plantarflexion, inversion/eversion, medial/lateral rotation. AB participants are reported in grey, while mean \pm SD of the AB group is reported in black. Values for participants with physical impairments are presented as mean \pm SD, with colors corresponding to the legend. The ankle angle is analyzed only in setup 1 and 2, and consequently, PartB and PartC are not included in the analysis.

Chapter 4 - Results and Discussion

		KNEE ROM [deg]			
		Flexion Extension		Medial Lateral rotation	
PartA AB group setup	1	119.1 ± 12.0		38.6 ± 8.2	
	2	20.9 ± 9.6		13.9 ± 4.5	
	2	21.9 ± 0.9		11.6 ± 1.0	

Table 15 - Range of Motion (ROM)of the knee, expressed in degree. Values are reported as mean ± SD. The knee angle is considered between the shank segment and the thigh segment.

		ANKLE ROM [deg]				
		Dorsiflexion Plantarflexion		Inversion Eversion		Medial Lateral rotation
PartA AB group setup	1	63.2 ± 11.4		12.7 ± 2.7		10.7 ± 3.8
	2	13.3 ± 4.8		2.0 ± 0.8		3.2 ± 1.2
	2	15.8 ± 0.6		1.6 ± 0.9		1.9 ± 0.4

Table 16 - Range of Motion (ROM)of the ankle, expressed in degree. Values are reported as mean ± SD. The ankle angle is considered between the foot segment and the shank segment.

Chapter 4 - Results and Discussion

Observing Figure 28 and Figure 29, it is evident that introducing movement constraints on the leg in setup 2 drastically decreases the range of motion (ROM) of the knee and ankle. Specifically, the most affected angle is the flexion/extension for the knee, also known as dorsiflexion/plantarflexion in the ankle. For the AB group, this angle decreases from 119.1 ± 12.0 deg to 20.9 ± 9.6 deg in the knee and from 63.2 ± 11.4 deg to 13.4 ± 4.8 deg in the ankle.

In other planes, such as medial/lateral rotation for the knee and inversion/eversion and medial/lateral rotation for the ankle, there is a decrease, but with less significance (Knee med/lat rot - Setup 1 38.6 ± 8.2 deg; Setup 2 13.9 ± 4.5 deg; Ankle inv/ever - Setup 1 12.7 ± 2.7 deg; Setup 2 2.0 ± 0.8 deg; med/lat rot Setup 1 10.7 ± 3.8 deg; Setup 2 3.2 ± 1.2 deg).

Participant A, in both the knee and ankle ROMs, mirrors the behavior of the AB group.

4.5 Joint's power

This section delves into the analysis of the power per stroke generated by each joint under consideration across the setups. While the details of the analyzed joint are expounded upon in section 3.4.9 *Kinetic data*, Table 17 succinctly summarizes the nomenclature and the distinction of the joints under scrutiny.

Chain		Joint	Convention adopted
1	Upper body	Elbow	Elbow
		Shoulder	Shoulder
		L5-S1 joint	L5-S1/T8 joint
		T8 joint	
2	Lower body	Hip	Hip
		Knee	Knee
		Ankle	Ankle

Table 17 – This table serves as a reminder of the conventions utilized to define power in the various joint. It provides a clear delineation of joints belonging to the upper and lower body. Additionally, it underscores the adopted convention for expressing power in both the L5-S1 joint and the T8 joint.

It is pertinent to highlight that the L5-S1 joint is exclusively considered in setups 1 and 2, while the T8 joint is considered in setups 3 and 4. To facilitate comprehension, these joints are presented together in the same graph.

The power associated to each joint across the setups is represented in two perspectives: relative power [%] and power generated [W]. Relative power signifies the percentage of power produced by the analyzed joint in relation to the total power generated. There are cases where obtaining a comprehensive understanding of the actual power values of the joints becomes crucial. This aids in identify whether variations in percentage across setups signify true differences in power or are a result of power reduction in other joints subject to movement constraints.

The following graphs divide the body into upper and lower parts, mirroring the distinction made to calculate the power using two distinct chains in section 3.4.9 *Kinetic Data*. Furthermore, the lower body analysis is confined to setups 1 and 2; for this reason only Participant A is represented.

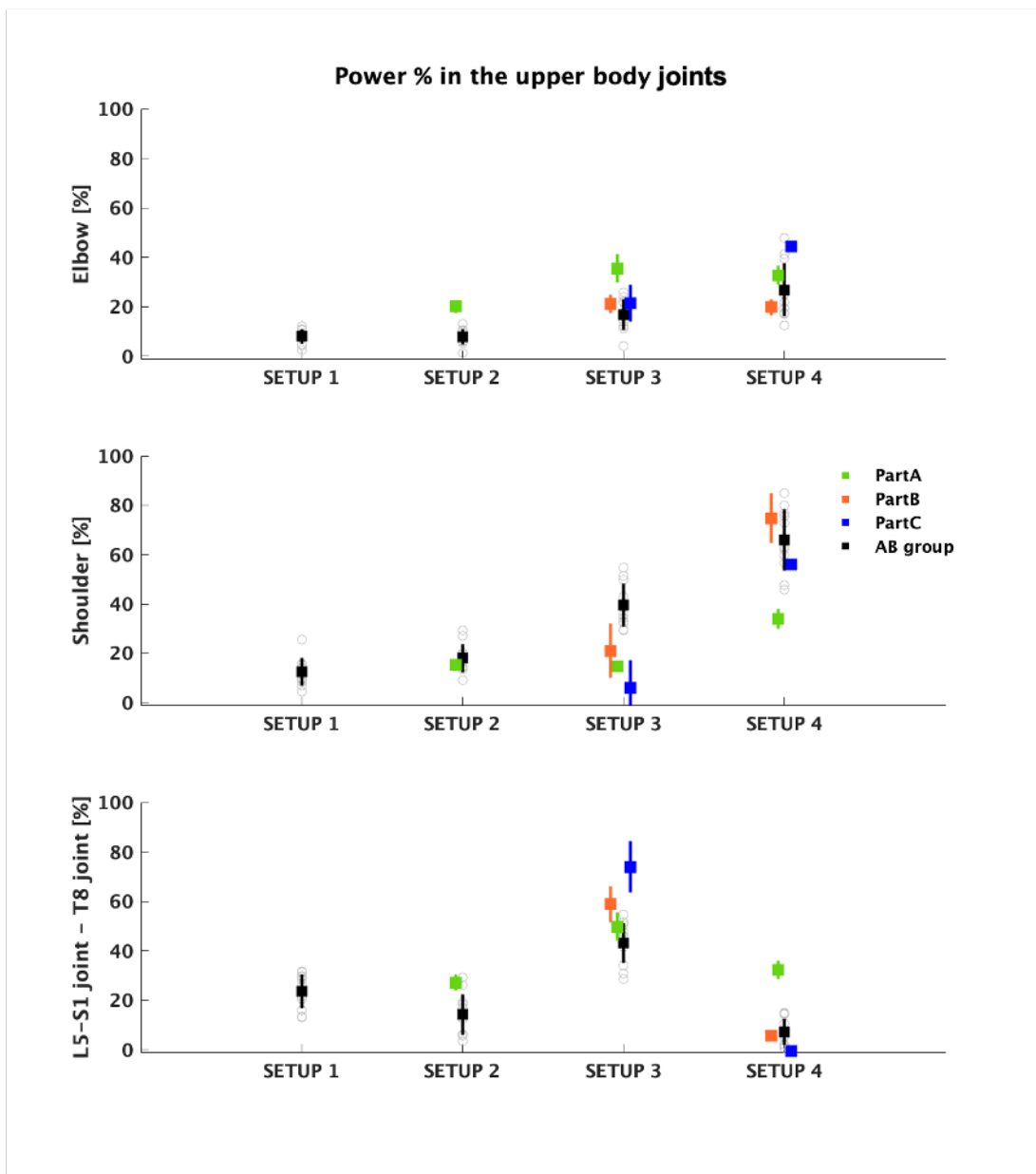


Figure 30 – Relative power in the upper body joints [%]: elbow, shoulder and L5-S1/T8 joint. AB participants are reported in grey, while mean \pm SD of the AB group is reported in black. Values for participants with physical impairments are presented as mean \pm SD, with colors corresponding to the legend.

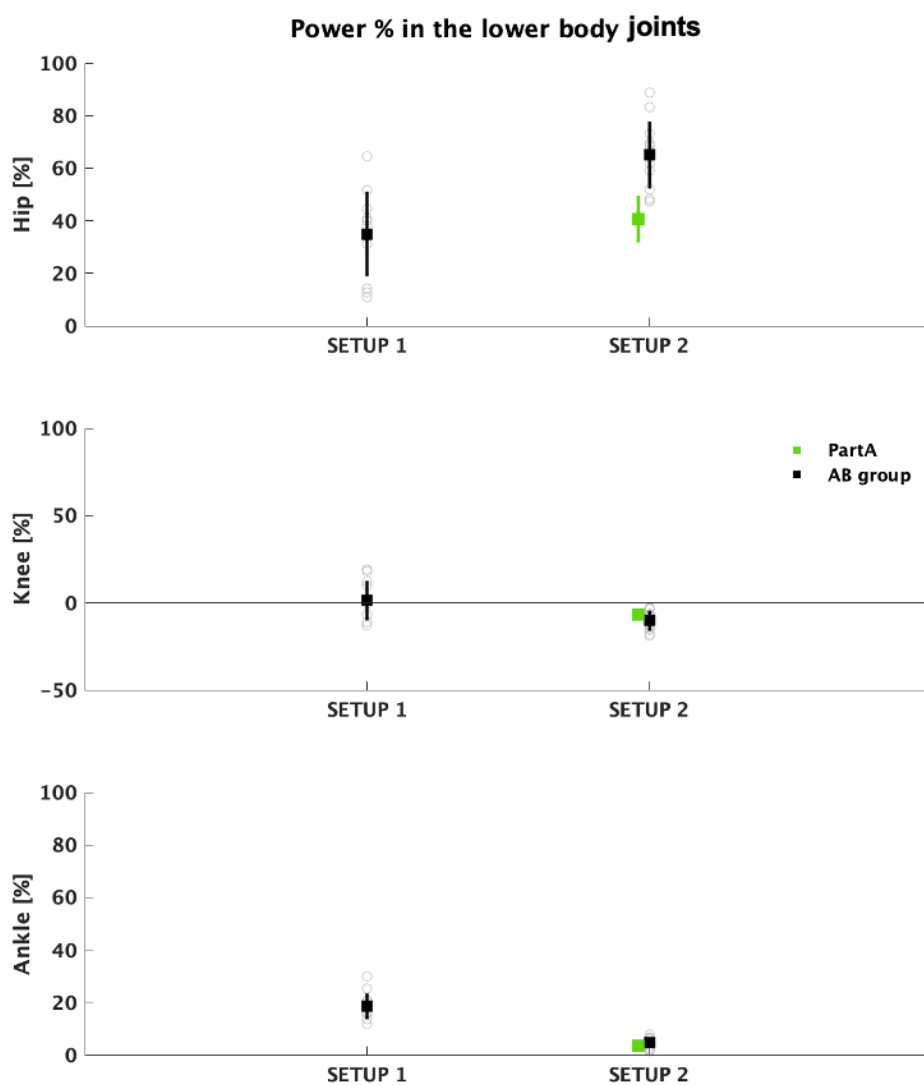


Figure 31 - Relative power in the lower body joints [Watt]: hip, knee and ankle. AB participants are reported in grey, while mean \pm SD of the AB group is reported in black. Values for participants with physical impairments are presented as mean \pm SD, with colors corresponding to the legend. The lower body is analyzed only in setup 1 and 2, and consequently, PartB and PartC are not included in the analysis.

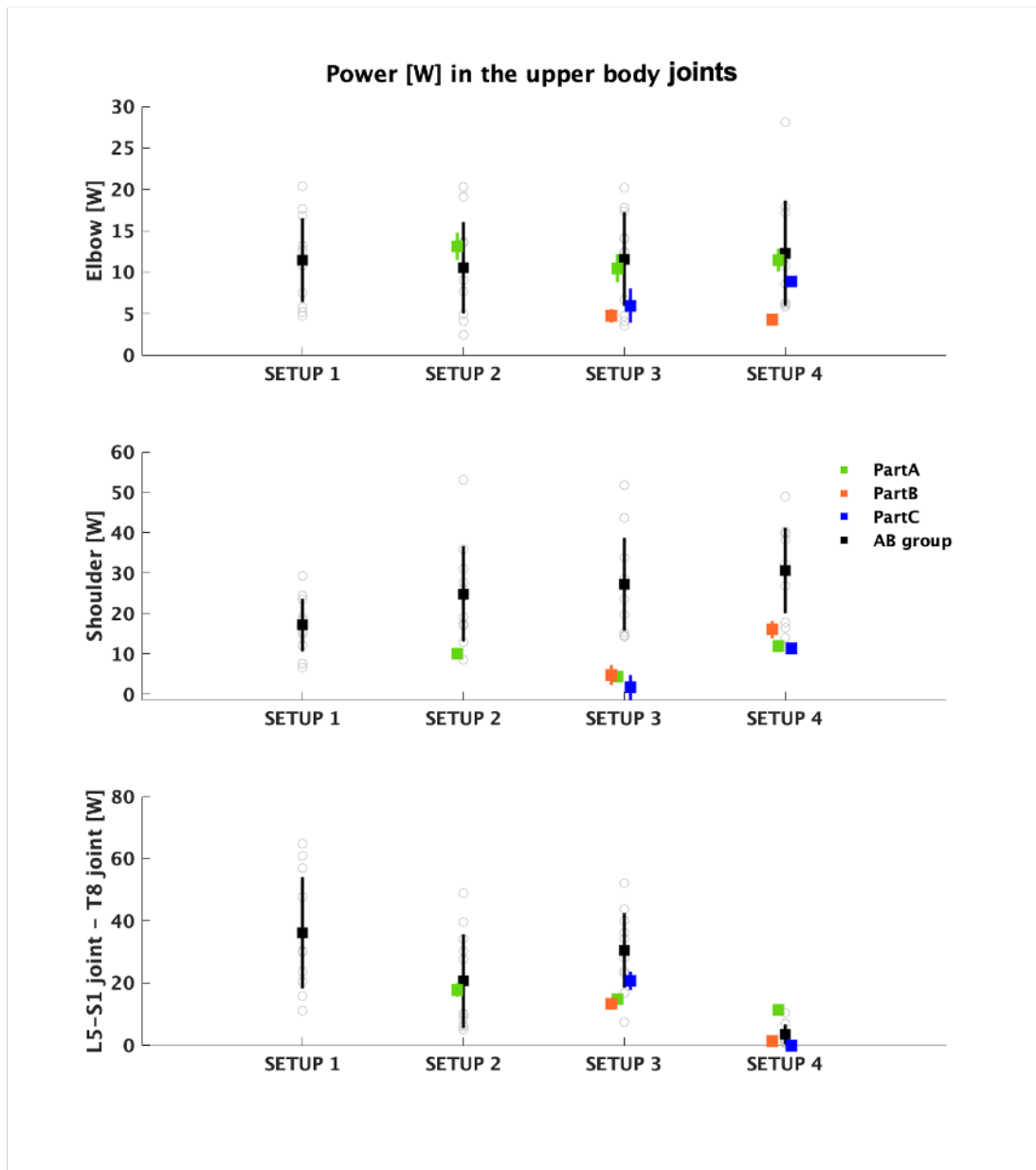


Figure 32 - Power in the upper body joints [Watt]: elbow, shoulder and L5-S1/T8 joint. AB participants are reported in grey, while mean \pm SD of the AB group is reported in black. Values for participants with physical impairments are presented as mean \pm SD, with colors corresponding to the legend.

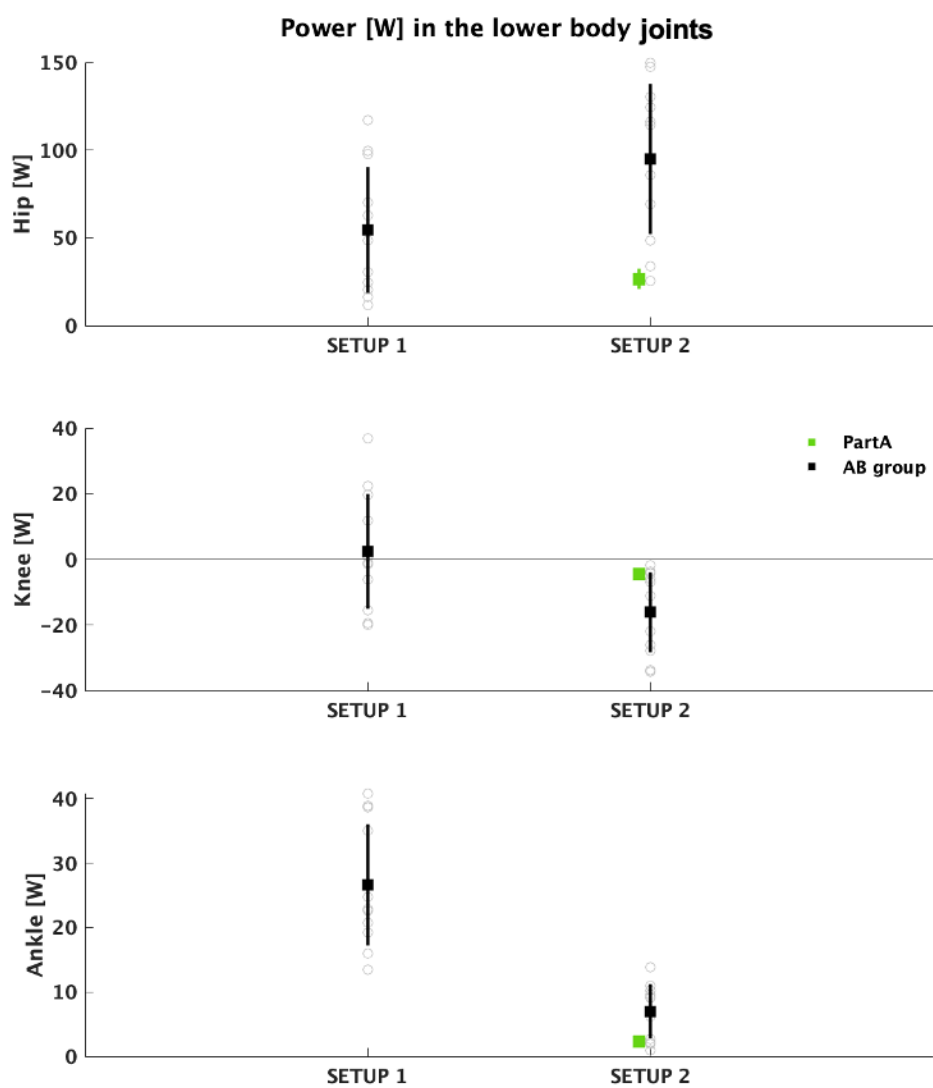


Figure 33 - Power in the lower body joints [Watt]: hip, knee and ankle. AB participants are reported in grey, while mean \pm SD of the AB group is reported in black. Values for participants with physical impairments are presented as mean \pm SD, with colors corresponding to the legend. The lower body is analyzed only in setup 1 and 2, and consequently, PartB and PartC are not included in the analysis.

Chapter 4 - Results and Discussion

		RELATIVE POWER [%]					
		ELBOW	SHOULDER	L5-S1/T8 joint	HIP	KNEE	ANKLE
AB group	1	8.1 ± 3.0	12.5 ± 5.5	23.8 ± 6.9	35.0 ± 16.0	1.3 ± 11.4	18.7 ± 5.0
	2	7.8 ± 3.2	18.1 ± 5.7	14.4 ± 8.2	65.0 ± 12.8	-10.3 ± 5.8	4.6 ± 2.0
	3	16.7 ± 6.0	39.5 ± 8.7	43.1 ± 8.2	-	-	-
	4	26.7 ± 10.8	66.2 ± 12.5	7.2 ± 5.3	-	-	-
PartA	2	20.2 ± 2.6	15.3 ± 1.9	27.3 ± 3.3	40.9 ± 8.9	-7.0 ± 1.7	3.6 ± 0.9
	3	35.3 ± 5.8	15.1 ± 2.2	49.7 ± 5.7	-	-	-
	4	32.2 ± 3.8	34.7 ± 4.3	31.9 ± 3.6	-	-	-
PartB	3	21.6 ± 3.8	20.7 ± 11.0	58.8 ± 7.4	-	-	-
	4	19.4 ± 3.3	74.8 ± 9.9	-	-	-	-
PartC	3	21.6 ± 6.0	6.3 ± 8.7	73.3 ± 8.2	-	-	-
	4	41.1 ± 0.5	58.7 ± 1.2	-	-	-	-

Table 18 – Relative power of the body joints, expressed in %. Values are reported as mean ± SD. Some L5-S1/T8 joint values in setup 4 are excluded from reporting due to being zero.

		POWER [W]					
		ELBOW	SHOULDER	L5-S1/T8 joint	HIP	KNEE	ANKLE
AB group	1	11.5 ± 5.1	17.2 ± 6.6	36.2 ± 17.9	54.6 ± 35.8	2.5 ± 17.5	26.7 ± 9.4
	2	10.6 ± 5.5	24.8 ± 11.8	20.6 ± 15.1	95.1 ± 42.8	-16.1 ± 12.1	7.0 ± 4.2
	3	11.6 ± 5.7	27.2 ± 11.5	30.5 ± 12.1	-	-	-
	4	12.3 ± 6.3	30.6 ± 10.6	3.5 ± 3.1	-	-	-
PartA	2	13.1 ± 1.7	10.0 ± 1.1	17.7 ± 2.2	26.6 ± 5.8	-4.5 ± 1.1	2.4 ± 0.6
	3	10.5 ± 1.7	4.4 ± 0.6	14.7 ± 1.7	-	-	-
	4	11.5 ± 1.4	12.0 ± 1.4	11.4 ± 1.3	-	-	-
PartB	3	4.8 ± 0.8	4.7 ± 2.5	13.2 ± 1.6	-	-	-
	4	4.2 ± 0.7	16.0 ± 2.1	-	-	-	-
PartC	3	6.0 ± 2.1	1.7 ± 3.1	20.6 ± 2.9	-	-	-
	4	8.9 ± 0.1	11.3 ± 0.2	-	-	-	-

Table 19 - Power of the body joints, expressed in Watt. Values are reported as mean ± SD. Some L5-S1/T8 joint values in setup 4 are excluded from reporting due to being zero.

Chapter 4 - Results and Discussion

The investigation into the impact of movement constraints on power production across different body joints and setups is a critical aspect of this study. The overarching hypothesis sets that constraints would likely lead to a reduction in power generated by lower body joints and the trunk, prompting compensatory adjustments in the power generated by the arms, specifically the elbow and shoulder. This represents a focal point in understanding power dynamics across setups.

In Figure 31 and Figure 33 a comprehensive representation of the power behavior for lower body joints, including the hip, knee, and ankle, during setups 1 and 2 is presented. As anticipated, the AB group undergoes a notable reduction in power output from the knee and ankle when transitioning from setup 1 (ankle: 26.7 ± 9.4 W; knee: 2.5 ± 17.5 W) to setup 2 (ankle: 7.0 ± 4.2 W; knee: -16.1 ± 12.1 W). However, intriguingly, the introduction of movement constraints on the sliding seat, impeding effective leg pushing, results in an increased power production by the hip (Setup 1: 54.6 ± 35.8 W; Setup 2: 95.1 ± 42.8 W). A noteworthy observation is the predominantly negative power produced by the knee, indicating power absorption and potential power transfer to the hip.

Graphical representations, incorporating power values in Watts and relative power (%), consistently portray the behavior of lower body joints. Notably, an increase in hip power from setup 1 ($35.0 \pm 16.0\%$) to setup 2 ($65.0 \pm 12.8\%$) is opposed to a decrease in power generated from the knee (Setup 1: $1.3 \pm 11.4\%$; Setup 2: $-10.3 \pm 11.8\%$) and from the ankle (Setup 1: $18.7 \pm 5.0\%$; Setup 2: $4.6 \pm 2.0\%$).

Particularly noteworthy is Participant A, the only participant with physical impairments in setup 2, exhibiting similar behavior to the AB group in the knee and ankle joints, both in values and percentages (PartA, knee: -4.5 ± 1.1 W, $-7.0 \pm 1.7\%$; ankle: 2.4 ± 0.6 W, $3.6 \pm 0.9\%$). However, in the hip joint in setup 2, Participant A demonstrates lower power than the AB group (PartA: $40.9 \pm 8.9\%$, 26.6 ± 5.8 W), despite showing a thigh ROM similar to the AB group. This validates Participant A's feedback, indicating a perceived

need for higher trunk and abdominal power during this setup, where some AB group individuals used their legs for balance. Surprisingly, despite expecting higher L5-S1/T8 joint power from the AB group, relative power is significantly higher for PartA ($27.3\pm 3.3\%$) compared to the AB group ($14.4\pm 8.2\%$), while power values are similar (PartA 17.7 ± 2.2 W, AB group 20.6 ± 15.1 W).

Shifting focus to the upper body, particularly on L5-S1/T8 joint relative power, a subtle decrease is observed for the AB group when increasing constraints, from setup 1 to setup 2 (Figure 30 and Figure 32): Setup 1: $23.8\pm 6.9\%$; Setup 2: $14.4\pm 8.2\%$. This decrease aligns with a reduction in power values (Setup 1: 36.2 ± 17.9 W; Setup 2: 20.6 ± 15.1 W), presenting an intriguing perspective in light of the ROM analysis, where trunk ROM increased from setup 1 to setup 2. This decrease might be a consequence of the increase in hip joint power. From setup 2 to setup 3, there is a noteworthy increase in the relative power produced by the L5-S1/T8 joint (Setup 3: $43.1\pm 8.2\%$). However, this increase is not proportionally reflected in power values where they increase less (Setup 3: 30.5 ± 12.1 W). Unsurprisingly, from setup 3 to setup 4, the imposition of constraints on trunk movement leads to a severe decrease in power produced by the L5-S1/T8 joint, nearly reaching zero for the AB group (Setup 4: $7.2\pm 5.3\%$, 3.5 ± 3.1 W).

This behavior across the setups is partially mirrored by participants with physical impairments. Notably, the main differences include Participant A in setup 4, where he continues to utilize the trunk more than the AB group (PartA: $31.9\pm 3.6\%$, 11.4 ± 1.3 W), evident in both power presentations and in the previous ROM analysis (PartA trunk flex/ext Setup 4: 19.0 ± 1.5 deg).

Additionally, participant C in setup 3, as a result of the previously assumed arm fatigue, presents higher relative power in the L5-S1/T8 joint (PartC: $73.3\pm 8.2\%$), caused by smaller relative power in the shoulder joint (PartC: $6.3\pm 8.7\%$, AB group: $39.5\pm 8.7\%$). However, the power value is within the AB group variance for the L5-S1/T8 joint (PartC: 20.6 ± 2.9 W),

Chapter 4 - Results and Discussion

whereas for the shoulder, it is smaller than the AB group (PartC: 1.7 ± 3.1 W; AB group: 27.2 ± 11.5 W).

In setup 3, participant B also exhibits some differences from the AB group, particularly in showing higher relative power of the L5-S1/T8 joint (PartB: $58.8\pm 7.4\%$). However, similar to participant C, the power value in Watts is smaller than the AB group (PartB: 20.6 ± 2.9 W).

The shoulder joint generally for the AB group exhibits an increase in relative power across setups, rising from $12.5\pm 5.5\%$ in setup 1 to $66.2\pm 12.5\%$ in setup 4. However, the power values reveal that although there is growth from setup 1 to setup 2 (Setup 1: 17.2 ± 6.6 W, Setup 2: 24.8 ± 11.8 W), thereafter, a consistent behavior is observed (Setup 3: 27.2 ± 11.5 W; Setup 4: 30.6 ± 10.6 W). This pattern is mirrored by the elbow, where relative power in setup 1 is $8.1\pm 3.0\%$, increasing to $26.7\pm 10.0\%$ in setup 4. Similar to the shoulder, the power value remains constant across setups (Setup 1: 11.5 ± 5.1 W; Setup 2: 10.6 ± 5.5 W; Setup 3: 11.6 ± 5.7 W; Setup 4: 12.3 ± 6.3 W). These observations regarding the behavior of the shoulder and elbow answer the question of whether there is compensation made by these joints. The analysis shows that there is no compensation across setups.

Participant A exhibits a different behavior from the AB group in the shoulder joint from setup 2 to setup 3. Notably, the expected behavior is an increase in power between these setups. However, he demonstrates no differences in relative power across these setups (Setup 2: $15.3\pm 1.9\%$; Setup 3: $15.1\pm 2.2\%$), indicating a decrease in power value from 10.0 ± 1.1 W in setup 2 to 4.4 ± 0.6 W in setup 3. This reduction in shoulder power is justified by a higher utilization of the trunk and elbow in setup 3 (Part A – L5-S1/T8 joint: $49.7\pm 5.7\%$; elbow: $35.3\pm 5.8\%$; AB group L5-S1/T8 joint: $43.1\pm 8.2\%$; elbow: 16.7 ± 6.0 %). This distinct use of the shoulder by Participant A is also evident in setup 4. In this case, he aligns with the AB group by increasing the relative utilization of the elbow and shoulder from setup 3 to 4 (Setup 4, PartA – elbow: $32.2\pm 3.8\%$; shoulder: $34.7\pm 4.3\%$). However, unlike the AB group, he also increases the power value in the shoulder while maintaining

Chapter 4 - Results and Discussion

consistent elbow utilization (Setup 3 elbow: 10.5 ± 1.7 W; shoulder: 4.4 ± 0.6 W; Setup. 4: elbow: 11.5 ± 1.4 W; shoulder: 12.0 ± 1.4 W).

Participant B's relative powers in the elbow and shoulder partially mirror the AB group, with the main difference being highlighted in setup 3, where she presents smaller relative power in the shoulder (PartB, Setup 3 – elbow: $21.6 \pm 6.0\%$; shoulder: $20.7 \pm 11.0\%$; Setup 4 – elbow: $19.4 \pm 3.3\%$; shoulder: $74.8 \pm 9.9\%$) . However, the behavior aligns with the AB group, and the power values produced by the elbow and shoulder are consistently smaller than those of the AB group. This difference might be attributed to a higher instability of the shoulder caused by Ehlers-Danlos syndrome [61-63].

As noted previously, Participant C, likely due to her physical impairment and the assumed higher muscular fatigue in the arms caused by the Spinocerebellar ataxia, performed by relying more on her trunk than her upper limbs in setup 3. (PartC: L5-S1/T8 joint: $73.3 \pm 8.2\%$, 20.6 ± 2.9 W; shoulder: $6.3 \pm 8.7\%$, 1.7 ± 3.1 W; elbow: $21.6 \pm 6.0\%$, 6.0 ± 2.1 W). Consequently, the relative power in the shoulder is significantly smaller compared to the AB group's, as is the absolute power value. However, in setup 4 (PartC: L5-S1/T8 joint: $\sim 0\%$; shoulder: $58.7 \pm 1.2\%$, 11.3 ± 0.2 W; elbow: $41.1 \pm 0.5\%$, 8.9 ± 0.1 W), her performance aligns more closely with the AB group, emphasizing that the observed difference in setup 3 is likely attributable to fatigue.

Based on these evaluations, it can be asserted that while there is no power compensation from the shoulder and elbow for the AB group, this is not the case for participants with physical impairments. Specifically, for all three participants, there is an increase in power in the shoulder from setup 3 to setup 4, indicating a significant divergence from the AB group.

Chapter 5

Conclusions

In conclusion, this research aimed to investigate biomechanical differences in rowing under varying movement constraints, with a specific focus on comparing individuals with and without physical impairments. The study revealed several key findings that contribute to our understanding of rowing mechanics and performance.

Firstly, an examination of performance indicated a reduction in handle force with increased movement constraints. Notably, participants without impairments exhibited diverse rowing techniques across setups, while those with physical impairments maintained more consistent patterns. The variations observed in technique underscore the non-professional rowing background of the participants.

Total power generated by rowers generally decreased across setups, with Participant A's anomalous increase in force during setup 4 suggesting a potential miscalculation of intensity in setup 3. Intriguingly, the decrease in power from setup 2 to setup 3 hinted at residual leg function disparities within the PR2 class.

Analysis of body segment range of motion (ROM) highlighted differences in the shoulder and trunk, closely linked and affected by movement constraints. While setups 1 to 2 saw increased ROM, setups 3 to 4 exhibited a decrease. Participants with physical impairments, particularly Participant B, demonstrated distinct 3D analysis-worthy variations, reflecting the influence of impairments on shoulder joint stability.

Chapter 5 - Conclusions

Power analysis of body joints showed an expected decrease in lower body joint power from setup 1 to setup 2. However, the upper body, particularly the shoulder and elbow, did not compensate for the decline in power across setups for the AB group. Notably, participants with physical impairments exhibited a slight increase in shoulder power, indicating a unique response.

In summary, the addition of movement constraints in rowing led to a reduction in performance, evident through diminished joint participation and force generation. The ROM of various body segments was affected by physical impairments, emphasizing the need for tailored training. Noteworthy differences were observed between setups 2 and 3, both categorized as PR2 class.

However, several limitations must be acknowledged. The absence of classified para-athletes and discrepancies in segment constructions between setups 1 and 2 versus setups 3 and 4, due to marker visibility issues, pose challenges in drawing definitive conclusions. These limitations underscore the need for further research and refinement of methodologies in studying the biomechanics of rowing, especially in populations with physical impairments.

Chapter 6

References

1. Aviron, R.C., *Para-rowing classification*. 2019.
2. Li, Y., et al., *Trunk and shoulder kinematics of rowing displayed by Olympic athletes*. Sports Biomechanics, 2020. **22**: p. 1-13.
3. Nauright, J., *Sports around the World: History, Culture, and Practice [4 volumes]: History, Culture, and Practice*. 2012: ABC-CLIO.
4. Secher, N.H. and S. Volianitis, *The Handbook of Sports Medicine and Science: Rowing*. 2009: Wiley.
5. Hofmijster, M.J., A.J. van Soest, and J.J. de Koning, *Rowing skill affects power loss on a modified rowing ergometer*. Medicine & Science in Sports & Exercise, 2008. **40**(6): p. 1101-1110.
6. Bartlett, R., *Introduction to sports biomechanics: Analysing human movement patterns*. 2014: Routledge.
7. Baudouin, A. and D. Hawkins, *Investigation of biomechanical factors affecting rowing performance*. Journal of biomechanics, 2004. **37**(7): p. 969-976.
8. Buckeridge, E., *Biomechanical asymmetries and joint loading in elite rowers*. 2013.
9. Bernstein, I., O. Webber, and R. Woledge, *An ergonomic comparison of rowing machine designs: possible implications for safety*. British Journal of Sports Medicine, 2002. **36**(2): p. 108-112.
10. Brearley, M.N., N.J.d. Mestre, and D.R. Watson, *Modelling the rowing stroke in racing shells*. The Mathematical Gazette, 1998. **82**(495): p. 389-404.
11. Cutler, B., et al., *Comparing para-rowing set-ups on an ergometer using kinematic movement patterns of able-bodied rowers*. J Sports Sci, 2017. **35**(8): p. 777-783.
12. Lamb, D.H., *A kinematic comparison of ergometer and on-water rowing*. The American journal of sports medicine, 1989. **17**(3): p. 367-373.
13. Vieira, T., et al., *Design and Test of a Biomechanical Model for the Estimation of Knee Joint Angle During Indoor Rowing: Implications*

Chapter 6 - References

- for FES-Rowing Protocols in Paraplegia*. IEEE Trans Neural Syst Rehabil Eng, 2018. **26**(11): p. 2145-2152.
14. Kleshnev, V., *Moving the rowers: Biomechanical background*. Aust. Rowing, 2002. **25**: p. 16-19.
 15. World Rowing FISA. *APPENDIX R15 – Para Rowing Classification Regulations. Event Regulations and/or Departures from the World Rowing Rules of Racing*. 2021; Available from: <https://www.paralimpicos.es/sites/default/files/inline-files/PARA%20ROWING%20CLASSIFICATION%20REGULATIONS%202021.pdf>.
 16. Paris 2024. *Para-Rowing*. 2023; Available from: <https://www.paris2024.org/en/sport/para-rowing/>.
 17. World Rowing FISA. *Rowing and Para-Rowing 2023*; Available from: <https://worldrowing.com/events/rowing-and-para-rowing/>.
 18. World Rowing FISA, *World Rowing Instructional Manual for Para-Rowing Physical Impairment Classification 2022*.
 19. Severin, A.C., et al., *Case Report: Adjusting Seat and Backrest Angle Improves Performance in an Elite Paralympic Rower*. Front Sports Act Living, 2021. **3**: p. 625656.
 20. Thornton, J.S., et al., *Rowing Injuries: An Updated Review*. Sports Medicine, 2017. **47**(4): p. 641-661.
 21. Barrett, R.S. and J.M. Manning, *Rowing*. Sports Biomechanics, 2004. **3**(2): p. 221-235.
 22. Caplan, N., A. Coppel, and T. Gardner, *A review of propulsive mechanisms in rowing*. Proceedings of the Institution of Mechanical Engineers, Part P: Journal of Sports Engineering and Technology, 2010. **224**(1): p. 1-8.
 23. Umar, M.A., et al., *Changes of drive to recovery ratio during 2000m ergometer rowing among junior national rowers*. Malaysian Journal of Movement, Health & Exercise, 2019. **8**(1): p. 33-43.
 24. Olympics games 2024. *Olympic games Paris 2024*. 2023; Available from: www.olympics.com/.
 25. British Rowing. *Adaptive Rowing*. 2023; Available from: <https://www.britishrowing.org/go-rowing/learn-to-row/adaptive-rowing/>.
 26. Rowing Australia. *Paralympic Games*. 2023; Available from: <https://rowingaustralia.com.au/international/paralympic-games/>.

Chapter 6 - References

27. Cerne, T., et al., *Differences between elite, junior and non-rowers in kinematic and kinetic parameters during ergometer rowing*. Hum Mov Sci, 2013. **32**(4): p. 691-707.
28. Murphy, A.J., et al., *The calibration and application of a force-measuring apparatus on the seat of a rowing ergometer*. Proceedings of the Institution of Mechanical Engineers, Part P: Journal of Sports Engineering and Technology, 2009. **224**(1): p. 109-116.
29. Cutler, B., et al., *Using Peak Vicon data to drive Classic JACK animation for the comparison of low back loads experienced during para-rowing*. International Journal of Human Factors Modelling and Simulation, 2015. **5**(2): p. 99-112.
30. Bezodis, I.N., et al., *A biomechanical comparison of initial sprint acceleration performance and technique in an elite athlete with cerebral palsy and able-bodied sprinters*. Sports Biomech, 2020. **19**(2): p. 189-200.
31. Lawton, T.W., J.B. Cronin, and M.R. McGuigan, *Strength, Power, and Muscular Endurance Exercise and Elite Rowing Ergometer Performance*. The Journal of Strength & Conditioning Research, 2013. **27**(7): p. 1928-1935.
32. Ettema, G., et al., *The role of stroke rate and intensity on rowing technique*. Sports Biomech, 2022: p. 1-22.
33. Hofmijster, M.J., et al., *Effect of stroke rate on the distribution of net mechanical power in rowing*. Journal of Sports Sciences, 2007. **25**(4): p. 403-411.
34. Borg, G.A., *Psychophysical bases of perceived exertion*. Medicine and science in sports and exercise, 1982. **14**(5): p. 377-381.
35. Severin, A.C. and J. Danielsen, *Rotation sequence and marker tracking method affects the humerothoracic kinematics of manual wheelchair propulsion*. J Biomech, 2022. **141**: p. 111212.
36. Veeger, H.E.J., *The position of the rotation center of the glenohumeral joint*. Journal of Biomechanics, 2000. **33**(12): p. 1711-1715.
37. Grewal, M.S., L.R. Weill, and A.P. Andrews, *Global positioning systems, inertial navigation, and integration*. 2007: John Wiley & Sons.
38. Crassidis, F.L.M.J.L., *Fundamentals of Spacecraft Attitude Determination and Control*. 2014.
39. Holton, J.R., J.A. Curry, and J.A. Pyle, *Encyclopedia of atmospheric sciences*. 2003, Amsterdam: Academic Press Amsterdam.

Chapter 6 - References

40. Kapanji, I., *The physiology of the joint: the elbow: flexion and extension*. London: Churchill Livingstone, 1970.
41. Gowitzke, B.A. and M. Milner, *Scientific bases of human movement*. 1988.
42. Rodgers, M.M., *Gait Analysis: An Introduction, ed 2*. Physical Therapy, 1997. **77**(7): p. 783.
43. Wu, G., et al., *ISB recommendation on definitions of joint coordinate systems of various joints for the reporting of human joint motion-- Part II: shoulder, elbow, wrist and hand*. J Biomech, 2005. **38**(5): p. 981-992.
44. Ge Wu, S.S., Paul Allard, Chris Kirtley, Alberto Leardini, Dieter Rosenbaum, Mike Whittle, Darryl D D'Lima, Luca Cristofolini, Hartmut Witte, Oskar Schmid, Ian Stokes; , *ISB recommendation on definitions of joint coordinate system of various joints for the reporting of human joint motion—part I: ankle, hip, and spine*. Journal of Biomechanics, 2002.
45. Bonnefoy-Mazure, A., et al., *Rotation sequence is an important factor in shoulder kinematics. Application to the elite players' flat serves*. Journal of Biomechanics, 2010. **43**(10): p. 2022-2025.
46. Creveaux, T., et al., *Rotation sequence to report humerothoracic kinematics during 3D motion involving large horizontal component: application to the tennis forehand drive*. Sports Biomechanics, 2018. **17**(1): p. 131-141.
47. Šenk, M. and L. Cheze, *Rotation sequence as an important factor in shoulder kinematics*. Clinical biomechanics, 2006. **21**: p. S3-S8.
48. Charalambous, C., *Repeatability of Kinematic, Kinetic, and Electromyographic Data in Normal Adult Gait*. Classic Papers in Orthopaedics, 2014: p. 399-401.
49. Davis, R.B., et al., *A gait analysis data collection and reduction technique*. Human Movement Science, 1991. **10**(5): p. 575-587.
50. Dumas, R., E. Nicol, and L. Chèze, *Influence of the 3D Inverse Dynamic Method on the Joint Forces and Moments During Gait*. Journal of Biomechanical Engineering, 2007. **129**(5): p. 786-790.
51. Dumas, R., R. Aissaoui, and J.A. de Guise, *A 3D Generic Inverse Dynamic Method using Wrench Notation and Quaternion Algebra*. Computer Methods in Biomechanics and Biomedical Engineering, 2004. **7**(3): p. 159-166.
52. Vaughan, C.L., B.L. Davis, and J.C. O'connor, *Dynamics of human gait*. (No Title), 1992.

Chapter 6 - References

53. Wu, G. and P.R. Cavanagh, *ISB recommendations for standardization in the reporting of kinematic data*. Journal of biomechanics, 1995. **28**(10): p. 1257-1262.
54. Leva, P.d., *ADJUSTMENTS TO ZATSIORSKY-SELUYANOV'S SEGMENT INERTIA PARAMETERS*. J Biomech, 1996.
55. De Leva, P., *Adjustments to Zatsiorsky-Seluyanov's segment inertia parameters*. Journal of biomechanics, 1996. **29**(9): p. 1223-1230.
56. van Ingen Schenau, G.J. and P.R. Cavanagh, *Power equations in endurance sports*. J Biomech, 1990. **23**(9): p. 865-81.
57. Brusse, E., et al., *Fatigue in spinocerebellar ataxia*. Patient self-assessment of an early and disabling symptom, 2011. **76**(11): p. 953-959.
58. Martinez, A.R., et al., *Fatigue and its associated factors in spinocerebellar ataxia type 3/Machado-Joseph disease*. The Cerebellum, 2017. **16**: p. 118-121.
59. Martins, C.R., et al., *Fatigue is frequent and severe in spinocerebellar ataxia type 1*. Parkinsonism & Related Disorders, 2015. **21**(7): p. 821-822.
60. Yang, J.-S., et al., *Ataxic severity is positively correlated with fatigue in spinocerebellar Ataxia type 3 patients*. Frontiers in neurology, 2020. **11**: p. 266.
61. Kitagawa, T., N. Matsui, and D. Nakaizumi, *Structured Rehabilitation Program for Multidirectional Shoulder Instability in a Patient with Ehlers-Danlos Syndrome*. Case Reports in Orthopedics, 2020. **2020**: p. 8507929.
62. Leonardis, J., et al., *Three-Dimensional Motion of the Shoulder Complex during Activities of Daily Living in Youths with Hypermobile Ehlers-Danlos Syndrome*. Archives of Physical Medicine and Rehabilitation, 2021. **102**(10): p. e109.
63. Rombaut, L., et al., *Joint position sense and vibratory perception sense in patients with Ehlers-Danlos syndrome type III (hypermobility type)*. Clinical Rheumatology, 2010. **29**: p. 289-295.